THESIS

CORRELATION OF HAS2-ASSOCIATED GENE DUPLICATIONS WITH BIOLOGICAL AGGRESSIVENESS OF MAST CELL TUMORS IN CHINESE SHAR-PEI DOGS

Submitted by

Alana Pavuk Garner

Department of Microbiology, Immunology, and Pathology

In partial fulfillment of the requirements

For the degree of Master of Science

Colorado State University

Fort Collins, Colorado

Fall 2013

Master's Committee:

Advisor: Anne Avery

Douglas Thamm
Randall Basaraba

Copyright by Alana Pavuk Garner 2013

All Rights Reserved

ABSTRACT

CORRELATION OF HAS2-ASSOCIATED GENE DUPLICATIONS WITH BIOLOGICAL AGGRESSIVENESS OF MAST CELL TUMORS IN CHINESE SHAR-PEI DOGS

Cutaneous mucinosis in Shar-Pei dogs is the result of excessive dermal hyaluronan, a protein associated with angiogenesis and tumor cell motility in multiple human and canine neoplasms. Cutaneous mucinosis in Shar-Pei has been associated with gene duplications upstream of the hyaluronic acid synthase 2 gene (HAS2). The objective of this study was to evaluate the relationship between HAS2, cutaneous mucinosis, and features of mast cell tumor (MCT) aggressiveness in Shar-Pei dogs. Biopsies of cutaneous MCTs from 149 Shar-Pei and 100 non-Shar-Pei were graded according to two schemes for canine cutaneous MCTs. Biopsies of the Shar-Pei MCTs were also evaluated for degree of cutaneous mucinosis, depth of invasion, and microvessel density (MVD). Shar-Pei and non-Shar-Pei MCTs were evaluated via qPCR for relative copy number of the gene duplication upstream of HAS2. The proportion of grade III tumors was significantly higher in Shar-Pei than the general canine population ($p=1.044e-11$), with no difference in average age at diagnosis. Shar-Pei biopsies had significantly higher HAS2-associated gene segment duplications than non-Shar-Pei ($p=1.128e-11$), and copy number was significantly associated with the development of grade III tumors ($p=0.0077$), mitotic index > or = 7 ($p=0.022$), and tumoral MVD ($p<0.05$). Relative copy number was not significantly associated with the degree of cutaneous mucinosis or depth of invasion. Our data suggest a relationship between HAS2 gene duplications and features of MCT aggressiveness in Shar-Pei dogs.

ACKNOWLEDGEMENTS

I would like to acknowledge and thank each and every member of my graduate committee, as well as the faculty and staff of the Department of Microbiology, Immunology, and Pathology, for their contributions to the success of this project. Specifically, I would like to thank Dr. Rob Burnett, Alex Burke, and Dr. Teckla Webb for their assistance with DNA extraction and PCR; Todd Bass and the Histology lab staff; Brad Charles for his help with immunohistochemistry; and Dr. Ann Hess for her statistical expertise and advice. Finally, I would like to thank my friends and family for their support, especially my husband, Glen, and my parents, Dan and Sandy Pavuk.

TABLE OF CONTENTS

LIST OF TABLES

LIST OF FIGURES

INTRODUCTION

Mast cell tumors (MCTs) are one of the most common tumors of canine skin and display a wide range of biological behaviors that can be hard to predict (Simoes, 1994). Chinese Shar-Pei dogs have been reported as being susceptible to more aggressive, higher-grade tumors than other breeds, with these aggressive MCTs occurring in Shar-Pei of a younger median age than other breeds (Miller, 1995). In a review article by Welle and colleagues in 2008, the average age of Shar-Pei with a MCT was 4 years, versus the overall canine average of 8-8.5 years of age (Welle, 2008). In one study of 802 canine cutaneous MCTs, 5 out of 18 tumors seen in Shar-Pei occurred in dogs less than two years of age, and all of them were grade III, whereas the other 5 dogs under 2 years of age (3 Boxers and 2 Cocker Spaniels) were all grade I or II (Miller, 1995). Many large prognostic studies have been conducted on canine cutaneous MCTs, typically without mention of variations in biological behavior between breeds (Patnaik, 1984; Simoes, 1994; Kiupel, 2005; Sfiligoi, 2005; Romansik, 2007; Thompson, 2011). This study is the largest evaluation of MCTs in Shar-Pei dogs to date, allowing a more detailed characterization of breed-specific factors that may affect MCT grade and explain the propensity for higher grade tumors.

The question that naturally follows is why Shar-Pei would have more aggressive MCTs than other dog breeds. Chinese Shar-Pei with wrinkly skin and a swollen muzzle, termed the “meat-mouth” phenotype, is the result of accumulation of hyaluronan in the extracellular matrix of the dermis (Zanna, 2008). If the accumulation of hyaluronan is excessive, the result is a condition known as cutaneous mucinosis, which is characterized by thickened alopecic skin that develops subcutaneous mucinous masses and frequent ulceration. A related condition, known as Shar-Pei Fever, and similar to Familial Mediterranean Fever in humans, causes recurrent severe systemic inflammation, which can predispose the patient to renal amyloidosis and renal failure (Olsson, 2011).

Hyaluronan, the primary component of the dermal mucin, is a linear, non-sulfated glycosaminoglycan produced in the plasma membrane of fibroblasts, cancer cells, and inflammatory

cells by one of three isoforms of hyaluronic acid synthase (HAS1, HAS2, and HAS3), and is degraded by one of several hyaluronidase enzymes (Itano, 2011). Therefore, increased dermal hyaluronan may be due to increased synthesis or decreased degradation in the skin. Reverse transcriptase PCR of cultured dermal fibroblasts from 13 Shar-Pei with cutaneous mucinosis revealed an increase in HAS2 mRNA with no change in HAS1, HAS3, or hyaluronidase expression when compared to normal canine skin, pinpointing increased production of hyaluronan due to increased expression of the HAS2 gene as the primary cause of cutaneous mucinosis (Zanna, 2008). A second study confirmed the over-expression of HAS2 in Shar-Pei with cutaneous mucinosis using Western blotting, and also demonstrated increased hyaluronan itself in the cultured fibroblasts (Docampo, 2011).

A subsequent investigation identified two unstable overlapping regions of canine chromosome 13 just upstream of the HAS2 gene (**Figure 1**) that showed a strong association with the cutaneous mucinosis and Shar-Pei fever phenotypes (Olsson, 2011).

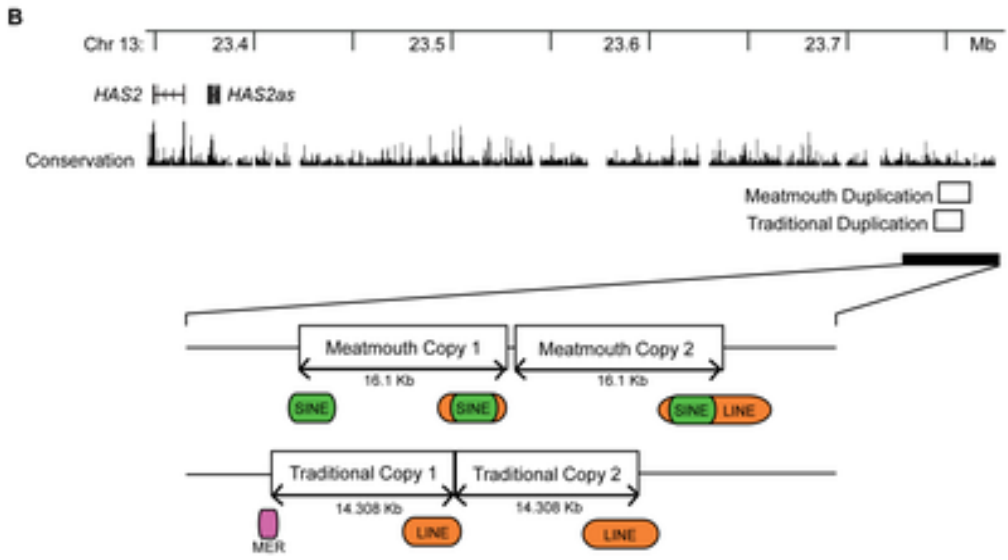

Figure 1. (from Olsson, 2011) **Meatmouth and traditional gene duplications.** Meathmouth and traditional gene duplications are overlapping segments located upstream of the HAS2 gene on chromosome 13 of the canine genome.

These two regions, named “meatmouth” and “traditional” after the phenotypic variation of skin wrinkling and swollen muzzle common in Shar-Pei in the United States versus traditional smooth-coated Shar-Pei seen more commonly in China (**Figure 2**), contain gene segment duplications unique to the Shar-Pei breed (Olsson, 2011).

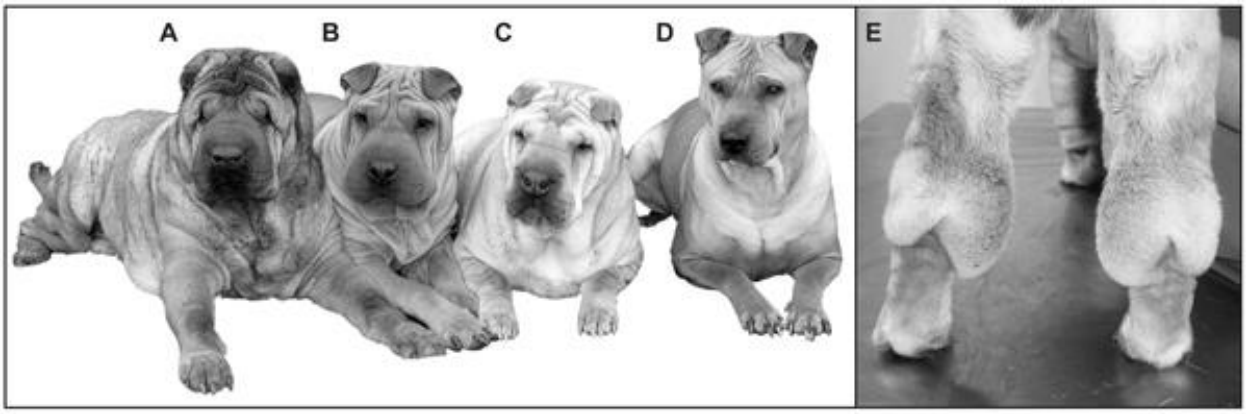

Figure 2. (from Olsson, 2011) **Shar-Pei skin phenotypes.** The “meatmouth” phenotype is seen in dogs A-C, with the “traditional” phenotypes in dog D. E displays cutaneous mucinosis commonly seen around the hocks of affected Shar-Pei.

An assay was developed to determine the gene duplication copy numbers for each dog, comparing real-time PCR amplification of the duplication loci to a single copy locus with ddCt statistical analysis (Olsson, 2011). Both the meatmouth copy number and the total copy number (containing both duplication segments) were significantly associated with the development of Shar-Pei Fever (**Figure 3)** (Olsson, 2011).

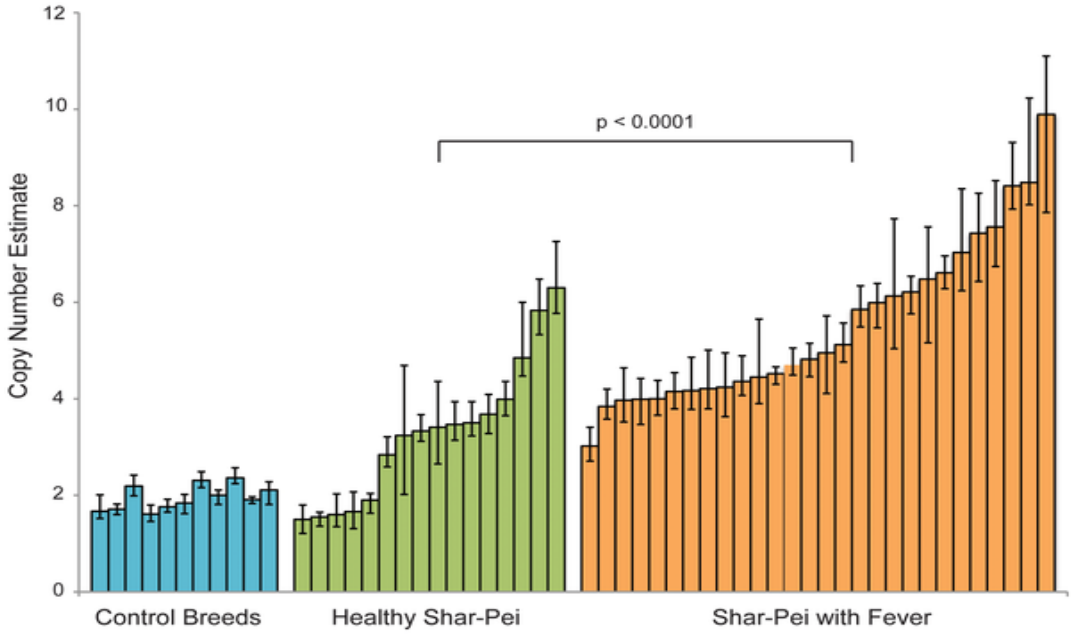

Figure 3. (from Olsson, 2011) **Copy number and Shar-Pei fever.** Higher relative meatmouth copy numbers are significantly associated with the development of Shar-Pei fever.

One of the goals of our study was to correlate the copy numbers determined by real-time PCR with the degree of cutaneous mucinosis (tissue levels of hyaluronan), and show that increased levels of both predict a higher-grade MCT in affected Shar-Pei dogs.

A further goal of this research was to explore how increased dermal hyaluronan may contribute to more aggressive biological behavior of the MCT. Hyaluronan itself promotes cell proliferation, cell motility, and angiogenesis; which contribute to tumor invasiveness and metastasis (Itano, 2011). High-molecular-weight hyaluronan helps retain water in the extracellular matrix, separating stromal collagen fibers, and making it easier for tumor cells and tumor-associated fibroblasts to migrate through dense connective tissue (Itano, 2011). Increased tumor and stromal hyaluronan have been significantly associated with canine colon tumors (Mukaratirwa, 2004), progression of canine transmissible venereal tumor (Mukaratirwa, 2004), and higher grade with decreased survival in human colon cancer (Ropponen, 1998). Mouse melanoma cells that had hyaluronan on the cell surface showed a higher metastatic frequency than hyaluronan-negative cells (Itano, 2011).

The HAS2 gene duplication copy number and tissue hyaluronan may also be associated with prognostic markers for canine cutaneous MCTs. Individual histologic criteria shown to be prognostically significant in canine cutaneous MCT include depth of invasion (Preziosi, 2007), mitotic index (Simoes, 1994; Preziosi, 2004; Romansik, 2007; Preziosi, 2007; Elston, 2009; Thompson, 2011) and cellular and nuclear morphology (Maiolino, 2005; Thompson, 2011). Angiogenesis, measured as intratumoral microvessel density, has also been shown to be prognostically significant in two studies of canine cutaneous mast cell tumors (Preziosi, 2004; Passantino, 2008; Poggiani 2012).

Based on the recent literature regarding increased HAS2 gene expression in Shar-Pei dogs with cutaneous mucinosis and Shar-Pei Fever, it follows that Shar-Pei dogs may have more aggressive MCT due to promotion of cell proliferation, invasion, and angiogenesis by dermal hyaluronan. Our goal was to demonstrate this relationship and increase understanding of molecular pathways of this common and important canine disease.

MATERIALS AND METHODS

Selection of cases and controls

Surgical biopsy specimens of 191 mast cell tumors (MCTs) from Shar-Pei (SP) dogs were collected from submissions to the Colorado State Veterinary Diagnostic Lab (VDL) between 2000 and 2010. Biopsies had been submitted by the Veterinary Teaching Hospital and outside practitioners from across the United States. 42 cases were excluded based on one or more of the following criteria: the MCT was located in tissue other than skin, the MCT was found in the subcutis only with no involvement of the overlying dermis, the diagnosis of MCT was not confirmed, or there were no formalin-fixed, paraffin-embedded (FFPE) blocks associated with the case in the diagnostic lab archives. All FFPE tissue blocks and hematoxylin and eosin (HE) slides were collected from the archives for each of the remaining 149 Shar-Pei MCT cases, as well as for 100 cutaneous MCTs from non-Shar-Pei dogs, 11 samples of normal skin from non-Shar-Pei dogs, and 13 samples of normal Shar-Pei skin submitted to the VDL between 2000-2010 to serve as controls. MCT-adjacent, tumor-free skin from 9 of the 149 Shar-Pei MCTs was also selected for further evaluation.

Comparison of age and grade of mast cell tumors from Shar-Pei and non-Shar-Pei dogs

The age at time of biopsy and MCT grade (Patnaik, 1984) for each of 100 SP MCTs and 100 non-SP MCTs were determined based on records from the VDL database. 5 non-SP MCTs and 3 SP MCTs were excluded because the tumors were located entirely within the subcutis.

DNA extraction from formalin-fixed paraffin-embedded tissue

20 um-thick tissue curls were cut from each MCT and control paraffin block for DNA extraction. At least 2 mm^2 of tissue was combined with 100 ul RNAse-free water (Qiagen, Valencia, California, USA), 10 ul 10X KAPA Express Extract Buffer, and 2 ul of 1U/ul KAPA Express Extract Enzyme from the KAPA

Express Extract DNA Extraction Kit with PCR Readymix in a 0.2 ml PCR tube (KAPA Biosystems, Inc., Woburn, Massachusetts, USA). DNA was extracted from each sample using the BIO-RAD iCycler version 4.006 (Bio-Rad Laboratories, Inc., Hercules, CA, USA) with the following extraction protocol: 75°C for 20 minutes, 95°C for 5 minutes, no hot start, 112 ul sample volume. The supernatant was transferred to a 0.2 ml PCR tube, then centrifuged at 14000 rpm for 3 minutes (Eppendorf Centrifuge 5417C , Eppendorf AG, Hamburg, Germany). Supernatant removal and centrifugation was repeated twice more. The supernatant containing extracted DNA was stored at 4°C for future use.

Determination of HAS2-associated gene duplication copy number via real-time PCR

Two primer sequences, named “Meat-mouth” and “Traditional” were designed to isolate and amplify gene segments corresponding to the gene duplications identified by Olsson and colleagues in 2011 (primers from Integrated DNA Technologies, Coralville, Iowa, USA; see **Table 1**). Two primer sequences known to amplify genes with no known duplications in dogs, MC1R2 and RE1, were also obtained to serve as single copy locus controls. A master mix for each primer was assembled, combining 10 ul SsoAdvanced SYBR Green Supermix (BioRad, Hercules, California, USA), 10 ul nuclease-free water (Qiagen, Valencia, California, USA), and 0.8 ul of the 10 uM primer pair solution for a final primer concentration of 400 nM for each qPCR reaction. Each sample was vortexed for 10 seconds.

Table 1. Primer pair nucleotide sequences

Primer Name	Primer Symbol	Sequence
"Meat-mouth"	MMF	5'-TTATGTTTTGCTGCCCTAGTCAGA-3'
	MMR	5'-ACCTGGCACCTGAGCAACTT-3'
"Traditional"	TradF	5'-TGCAGTTGTCATGTCGCAA-3'
	TradR	5'-TGGAGTGATTCGTTGGTTTCT-3'
Melanocortin-1 Receptor (single copy locus control)	MC1RF2	5'-TGCAACTCCATCATTGACCCCTT-3'
	MC1RR2	5'-CAGCCTCACCAGGAACATAGCAC-3'
Restrictive Element 1 (single copy locus control)	Re1F	5'-CCCATCAACTTCCTCACGCTCT-3'
	Re1R	5'-GTGAAGCCACCGAAGACCAT-3'

For each triplicate reaction, 3.5 ul of test DNA, control DNA, or nuclease-free water (no-template controls) was added to 70 ul master mix. The samples were vortexed for 10 seconds and centrifuged at 14000 rpm for 2 minutes (Eppendorf Centrifuge 5417C , Eppendorf AG, Hamburg, Germany). 20 ul for each technical triplicate were pipetted into a 96-well PCR plate, and the PCR amplification was performed using the BIO-RAD C1000 Thermal Cycler with CFX96 Real-Time System according to the manufacturer's protocol for use with the Sso Advanced SYBR Green Supermix (BioRad, Hercules, California, USA). Briefly, the samples underwent initial denaturation at 98°C for 2 min, followed by 40 cycles of denaturation at 98°C for 5 sec and annealing at 60°C for 15 sec, with a final melt curve of 65-95°C in 0.5°C increments every 3 seconds. Non-Shar-Pei MCT controls were included on each plate to ensure adequate PCR enzyme function, and consisted of DNA extracted (using the above protocol) from clinical samples received by the Colorado State University Clinical Immunology Laboratory. Since many different nSP MCT controls were used over the course of the study, overlap between controls on at least one plate allowed normalization. No-template controls were also included on each plate to evaluate master mix contamination.

Validation of a qPCR assay to determine HAS2 gene duplications

To verify that the SsoAdvanced SYBR Green Supermix (Bio-Rad) was able to amplify DNA extracted from FFPE MCTs without significant enzyme inhibition by heparin or formalin fixation, qPCR results from two lymph node aspirates of canine lymphoma and two FFPE lymph nodes with canine lymphoma were compared to two aspirated MCTs and two FFPE MCTs using the methods described above.

A serial dilution curve was then performed to validate the use of the ddCt statistical method of relative gene copy number quantification. qPCR was performed as described above using all four primer pairs on non-Shar-Pei FFPE MCT control DNA at dilutions of 10^{0} to 10^{-4} and a no-template control (Livak, 2001).

Grading and histologic evaluation of tumor features

A representative 5um-thick HE-stained tissue section containing a large cross-section of the tumor and abundant skin flanking the tumor was evaluated for each of the 149 SP MCT biopsies. Each tumor was re-graded by a single pathologist (APG) without prior knowledge of breed or previously-assigned grade, using both the grading scheme established by Patnaik in 1984, and the two-tiered grading system proposed in 2011 (Kiupel, 2011), eliminating inter-pathologist variation (Northrup, 2005). Grading was based on the published features described in **Tables 2 and 3**.

Table 2. Microscopic features used for grading of canine cutaneous mast cell tumors, Patnaik, 1984

Patnaik grading scheme		
Grade I	Grade II	Grade III
1. Neoplastic cells are within the dermis and interfollicular spaces 2. Well-differentiated mast cells are in rows or small groups, separated by mature collagen 3. Cells are monomorphic with ample cytoplasm 4. Most cells have distinct cell borders and medium-sized intracytoplasmic granules 5. Nuclei are round with condensed chromatin 6. Mitoses are absent 7. Minimal edema and necrosis are within traumatized tumors	1. Tumor is moderately to highly cellular 2. Neoplastic cells In deep dermis and subcutis into skeletal muscle 3. Cells are moderately pleomorphic with thin fibrovascular stroma to thick hyalinized stroma 4. Cells are round to ovoid with scattered spindle and giant cells 5. Cells have distinct cytoplasm with fine intracytoplasmic granules or indistinct cytoplasm with large hyperchromatic granules 6. Nuclei are round to indented with scattered chromatin and single nucleoli 7. Occasional cells are binucleated 8. Mitoses are rare (0-2/hpf) 9. Areas of diffuse edema and necrosis exist	1. Tumor is highly cellular and pleomorphic 2. Neoplastic tissue replaces the subcutis and deep tissues 3. Cells are medium-sized, round, ovoid, or spindloid in closely packed sheets 4. Cells have indistinct cytoplasm with fine intracytoplasmic or indistinct granules 5. Stroma is fibrovascular or thick and hyalinized 6. Nuclei are indented to round and vesiculated with one or more prominent nucleoli 7. Binucleated cells, giant cells, and scattered multinucleated cells are common 8. Mitoses are common (3-6/hpf) 9. Edema, hemorrhage, and necrosis within the tumor are common

Table 3. Microscopic features used for grading of canine cutaneous mast cell tumors, Kiupel, 2011

Two-tiered grading scheme	
Low-grade	High-grade
Tumor does not have any of the criteria of high-grade tumors	Tumor displays any one of the following: 1. Frequent mitoses (at least 7/10 hpf) 2. At least 3 multinucleated cells in 10 hpf 3. At least 3 bizarre nuclei in 10 hpf 4. Karyomegaly (At least 10% of neoplastic cells vary by at least 2-fold)

Evaluation criteria also included features determined to be prognostically significant alone or as part of a published grading scheme. Criteria included depth of invasion, cell pattern, cellular differentiation, nuclear typia, and karyomegaly scored according to the rubric adapted from the literature, and presented in **Table 4** and **Figures 4 and 5**. (Preziosi, 2007; Kiupel, 2011). Mitotic index was determined as the number of mitotic figures in the ten 400x hpf with the highest mitotic activity. Each ordinal subgroup of a subjective criterion was assigned a representative numerical score (1-4) to aid in statistical analysis.

Table 4. Criteria for histologic slide evaluation of Shar-Pei MCT (non-continuous variables)*

Depth of Invasion	Cell Pattern	Cellular Differentiation	Nuclear typia	Karyomegaly (Kiupel, 2011)
1:*Non-invasive*: confined to superficial dermis and interfollicular spaces	***1:****Type a:* rows or small groups of cells separated by mature collagen fibers of the dermis	***1:***Round and monomorphic with ample cytoplasm, distinct cytoplasmic boundaries, medium-sized granules, well granulated mast cells	***1:****Typical*: nuclei round and monomorphic with a condensed chromatin pattern	*Low*: Nuclear diameter of less than 10% of neoplastic cells vary by at least 2-fold
2:*Moderately invasive*: lower dermal and limited subcutaneous tissue invasion	***2:****Type b*: moderate to high cellularity in large groups with thin fibrovascular stroma	***2:***Round to ovoid, scattered spindle and giant cells, moderate anisocytosis and fine cytoplasmic granularity	***2:****Intermediate*: Nuclei moderately pleomorphic, round to indented, and with irregular chromatin, single prominent nucleolus	*High*: Nuclear diameter of at least 10% of neoplastic cells vary by at least 2-fold
3:*Highly invasive*: Massive infiltration of subcutaneous and deep tissue	***3:****Type c*: high cellularity in closely packed sheets with thick fibrovascular stroma that replaced most of subcutaneous and deep tissues	***3:***Marked anisocytosis, pleomorphic round, ovoid, or spindle, giant cells and scattered multinucs, indistinct and poorly granulated cytoplasm	***3:****Atypical*: Nuclei pleomorphic and one or more large prominent nucleoli	

*Adapted from Preziosi, 2007 (from Patnaik, 1984) unless otherwise noted

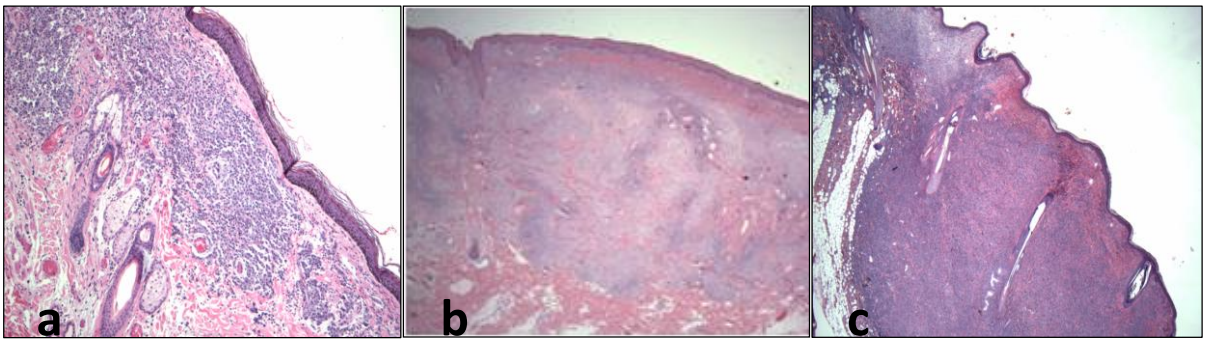

Figure 4. Criteria for histologic slide evaluation. Sections from Shar-Pei skin biopsies. (a) MCT is confined to the superficial dermis. HE, 200x (b) MCT extends to the deep dermis. HE, 100x (c) MCT extends deep into the subcutis. HE, 100x

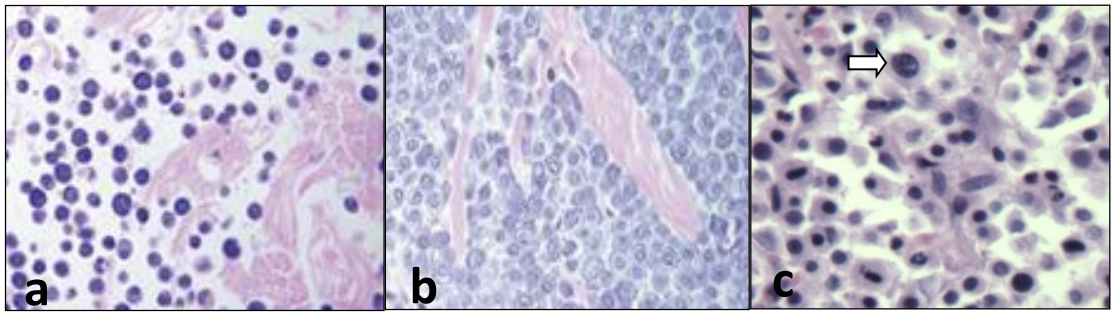

Figure 5. Additional criteria for histologic slide evaluation. HE, 400x (a) MCT with small groups of well-granulated mast cells separated by mature collagen of the dermis. (b) MCT with high cellularity, fine granularity, and thin fibrous stroma. (c) MCT with marked cellular and nuclear pleomorphism, poor granularity, and karyomegaly indicated by the open arrow.

Cutaneous mucinosis scoring via light microscopy

A representative HE tissue section from each of 149 SP MCTS and 33 SP and non-SP controls was evaluated to determine the degree of cutaneous mucinosis. Separation of dermal collagen bundles by mucin flanking, but not within, the tumor was scored using a novel scoring system. Each biopsy was assigned a score of 0 (0% expansion of the dermis by pale basophilic stippled extracellular matrix [mucin]), 1 (1-10% expansion of the dermis by mucin), 2 (>10-20% expansion of the dermis by mucin), or 3 (>20% expansion of the dermis by mucin), as demonstrated by **Figure 6** below.

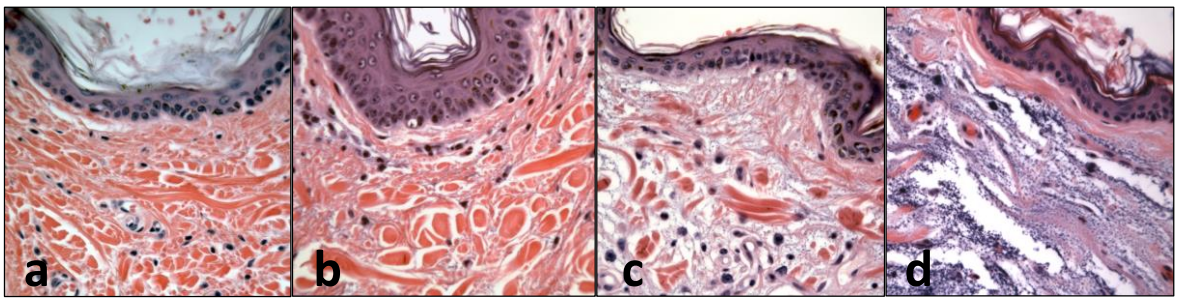

Figure 6. Mucin scoring method. Sections from MCT-adjacent Shar-Pei skin. HE, 400x. (a) 0: 0% expansion of dermis; (b) 1: 1-10% expansion of dermis by basophilic stippling; (c) 2: >10-20% expansion of dermis; (d) 3: >20% expansion of dermis.

Determination of tumor microvessel density via immunohistochemistry and light microscopy

Twenty-five low-grade (also Patnaik grade I or II) and 25 high-grade (also Patnaik grade III) Shar-Pei cutaneous MCTs were selected randomly for evaluation of tumor microvessel density. Sample numbers for each group were based on statistical power calculations using the Russ Lenth online power calculator (Lenth, 2009). For each case, additional tissue sections from the same block as the slides evaluated by light microscopy were sectioned at 5 µm thickness and mounted on charged slides. Tissue slides were dried in a 62° Celsius oven for 20 minutes, then placed in a Leica BOND-MAX fully automated stainer (Leica Microsystems, Buffalo Grove, Illinois, USA) for the remaining steps, as follows. The slides were deparaffinized to water, and heat-induced epitope retrieval was performed for 20 minutes using Bond Epitope Retrieval Solution 2 (pH 9.0) (Leica Biosystems Newcastle Ltd, Newcastle Upon Tyne, United Kingdom). A rabbit polyclonal antibody against human von Willebrand factor (previously known as Factor VIII-related antigen) at a 1:1,000 dilution was applied to tissue sections for 30 minutes at room temperature (Dako, Carpinteria, California, USA). Bound antibody was detected with addition of a secondary antibody (Bond Polymer AP anti-rabbit IgG, Leica Biosystems Newcastle Ltd, Newcastle Upon Tyne, United Kingdom) for 25 minutes, followed by Bond Polymer Refine Red Detection kit for 15 minutes, and counterstained with hematoxylin for 5 minutes according to the Leica RBT RED protocol (Leica Biosystems Newcastle Ltd, Newcastle Upon Tyne, United Kingdom). Duplicate tissues used as negative controls were processed similarly, with the substitution of normal control serum for the primary antibody (Bond Ready-to-Use Negative Control, Negative (Rabbit), Leica Biosystems Newcastle Ltd, Newcastle Upon Tyne, United Kingdom).

Similar to the method described by Preziosi (2004) for determining microvessel density within mast cell tumors, the tumor regions with the most dense immunoreactive vessels were identified at low power (40x), and the intratumoral MVD was reported as the total number of immunopositive cell

clusters counted in five high-powered fields (400x). Light microscopy was performed using an Olympus BH-2 microscope with WHK 10x/20 L oculars. Each 400x field was 0.196 mm^2.

Determination of tumor microvessel density by computer image analysis

Each of the immunohistochemically-stained slides of the 25 high-grade and 25 low-grade MCTs evaluated for tumor microvessel density by hand-scoring were also analyzed via computer image analysis. The tumor regions with the most dense immunoreactive vessels were identified at low power (40x), and five 400x images were captured per slide using an Olympus Q-Color3 camera attached to an Olympus BX40 microscope with Olympus Plan lenses and WH10x-H/22 oculars. The images were processed and saved using Olympus QCapture x64 version 2.9.12 computer software (Olympus, Melville, New York, USA). Each image captured of a 400x field was 0.0972 mm^2; therefore, microvessel density measurements were standardized to 0.196 mm^2 to allow for easy comparison between light microscopic and computer image analyses.

The captured images were analyzed using ImageJ version 1.46r, a free image analysis program produced by the NIH (imagej.nih.gov.ij, National Institutes of Health, Bethesda, Maryland, USA). A macro was written using the ImageJ macro recorder to analyze images consistently, and consisted of adjusting the color threshold of RBG images to exclude blue shades over 105, thus eliminating most of the hematoxylin counterstaining. The thresholded images were then converted to binary black and white images for further analysis. A size threshold was set to exclude clusters of less than 1000 pixels to eliminate non-endothelial nuclei that were not removed by the color thresholding. Finally, holes were filled to allow for inclusion of vessel lumina in the calculation of percent area of the image comprising vessels **(Figure 7)**. Measurements collected included: count (number of discrete positive shapes in image), total area (total number of positive pixels in image), average size (average number of pixels per positive shape), and area fraction (total area of positive shapes divided by total area of image). All

images to be analyzed were batched into a single folder, and the image analysis was run automatically to process all 250 images.

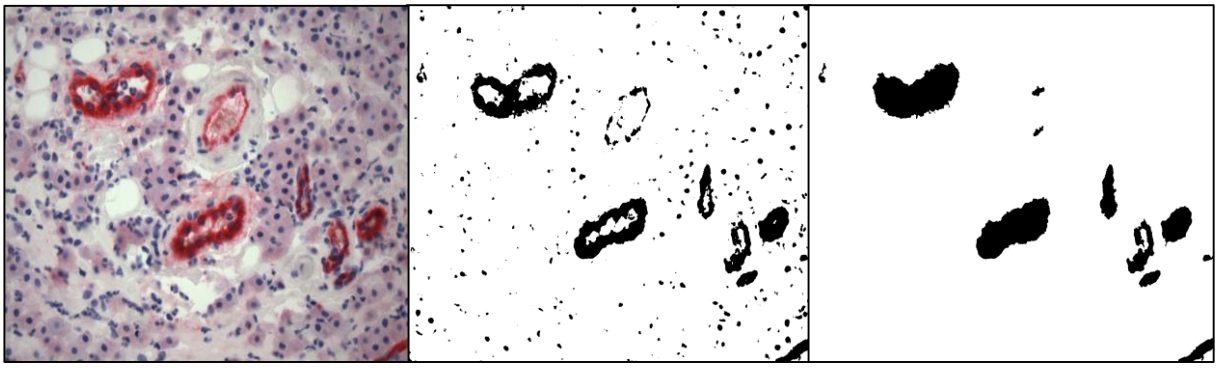

Figure 7. MVD computer image processing method. ImageJ, NIH**.** Shar-Pei MCT biopsy. (a) 400x image of FVIIIra IHC-stained slide. (b) Same image as in (a) after color thresholding. (c) Same image as in (b) after size thresholding.

Statistical analyses

The Russ Lenth online power calculator was used to determine that 25 MCTs per group were needed to have a 90% likelihood of detecting a true difference in mucinosis scores and MVD between low- and high-grade MCTs (Lenth, 2009). Power calculations also indicated that 50 MCTs were needed to have a 90% likelihood of detecting a true correlation of r=0.5. All subsequent statistical analysis was performed using R statistical software (Version 2.15.1, The R Foundation for Statistical Computing)

A Wilcoxon rank sum test was used to determine if there is a significant ($p<0.05$) difference in mean copy number or MVD between Grade I/II (low-grade) MCTs and Grade III (high-grade) MCTs, or if there is a significant ($p<0.05$) difference in mean copy number between tumors stratified by depth of invasion. The Wilcoxon rank sum test was also used to test the assumptions that Shar-Pei have higher copy numbers in normal skin than non-SP dogs and that copy numbers are the same in SP MCTs and adjacent tumor-free skin. A Kruskal-Wallis rank sum test and pairwise Wilcoxon for nonparametric data was used to determine if there is a significant ($p<0.05$) difference in copy number, mitotic index, or MVD

between MCTs stratified by mucin score. A Fisher's exact test was used to determine if there is a significant ($p<0.05$) relationship between mucin score and depth of invasion or grade. A Pearson r correlation was used to determine if there is a correlation between copy number and mitotic index, or between copy number and MVD.

The ddCt method, described by Livak in 2001, was used to evaluate each qPCR sample to determine the relative copy number of the "meat-mouth" and "traditional" gene duplications upstream of HAS2. In summary, as demonstrated graphically below in **Figure 8**, the difference between the C_t values for the "meat-mouth" and "traditional" amplicons and the average of the single copy loci for each sample were compared to the difference between the C_t values for the "meat-mouth" and "traditional" amplicons and the average of the single copy loci for the control, $-ddCT = dCT_{sample} - dCT_{ctrl}$. Results from multiple tests of one sample and primer were averaged. Results for both "meat-mouth" and "traditional" primers were averaged to assign a relative copy number for each dog.

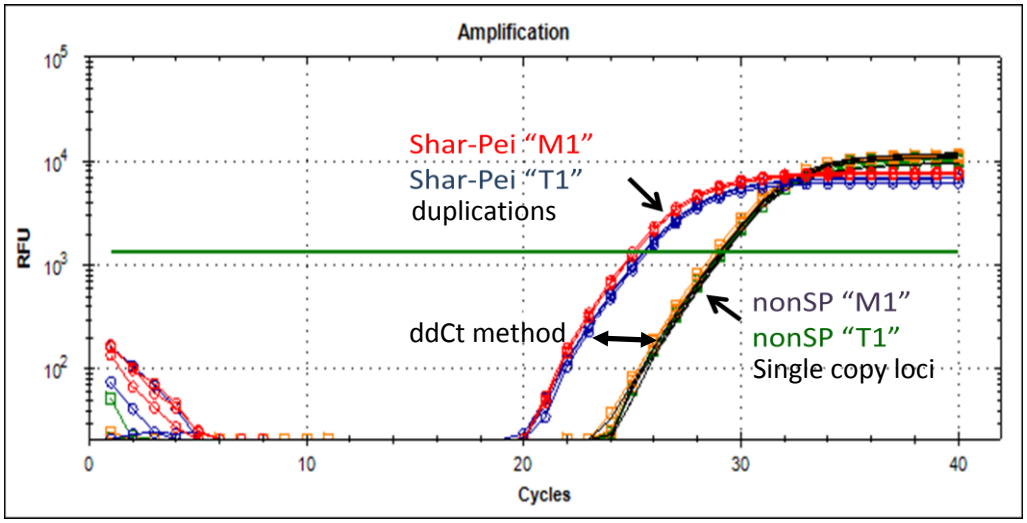

Figure 8. ddCt method of determining relative gene duplication copy numbers. The difference between the C_t values for the "meat-mouth" (red) and "traditional" (blue) amplicons and the average of the single copy loci (black) for each sample were compared to the difference between the C_t values for the "meat-mouth" (orange) and "traditional" (green) amplicons and the average of the single copy loci for the control (black).

RESULTS

Shar-Pei dogs develop higher-grade mast cell tumors than the general canine population, but not at a younger age

We first tested the hypothesis that Shar-Pei dogs develop MCTs of a higher grade and at an earlier age than other dogs. The age at time of biopsy and MCT grade (Patnaik, 1984) for each of 97 SP MCTs and 95 non-SP MCTs were determined based on records from the CSU-VDL database. As shown in **Figure 9** below, of SP MCTs, 3 were Grade 1 (3.1%), 52 were Grade 2 (53.6%), and 42 were Grade 3 (43.3%). Of non-SP MCTs, 21 were Grade 1 (22.1%), 69 were Grade 2 (72.6%), and 5 were Grade 3 (5.3%). Using the Fisher's exact test, grade and breed were not found to be independent ($p=1.044x10^{-11}$), suggesting that Shar-Pei dogs have a disproportionately higher number of high-grade tumors than the general canine population.

As shown in **Figure 10** below, the median age at time of diagnosis for both Shar-Pei and non-Shar-Pei dogs was 8 years, with no statistical difference between the groups as confirmed by the Welch two-sample t-test ($p=0.7987$). This suggests that Shar-Pei dogs do not develop mast cell tumors at a younger age than the general canine population.

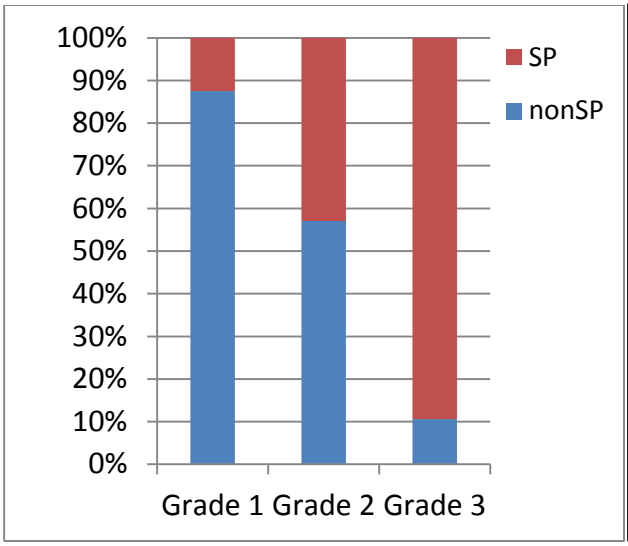

Figure 9. Percent of MCTs within each grade from 100 Shar-Pei and 100 non-Shar-Pei dogs

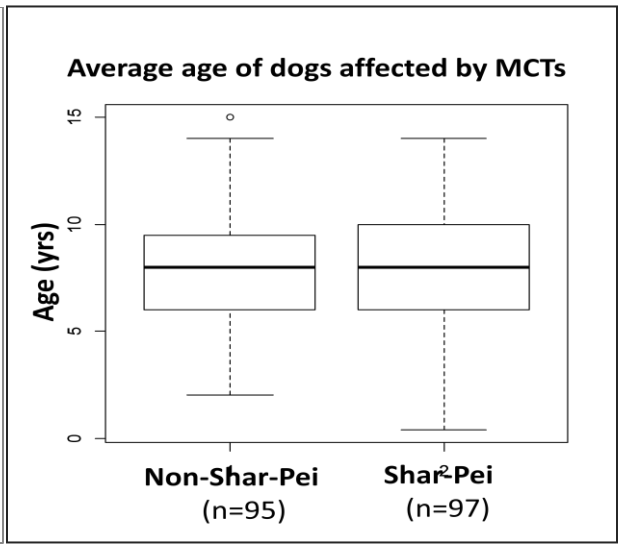

Figure 10. Comparison of median ages at time of diagnosis between Shar-Pei and non-Shar-Pei MCTs

qPCR is a valid assay to determine HAS2 gene duplications in FFPE MCT biopsies

Heparin and formalin fixation are known to inhibit some methods of DNA extraction and PCR amplification of DNA and RNA. To verify that the SsoAdvanced SYBR Green Supermix (Bio-Rad) was able to amplify DNA extracted from MCTs without significant enzyme inhibition by the heparin within mast cells, a lymph node aspirate of non-Shar-Pei canine lymphoma was compared to two aspirates of non-Shar-Pei canine mast cell tumors in two separate experiments, using the "traditional" and MCR2 primers run in duplicate. As shown in **Figure 11**, the Ct values for the lymphoma sample in red ranged from 24.09 to 24.27 cycles, the first MCT sample in blue ranged from 24.22 to 24.29 cycles, and the second MCT sample in pink ranged from 29.31 to 30.04 cycles, all within the accepted range of less than 39 cycles, with similar results between the two experiments (Bustin, 2009). The successful amplification of DNA from canine mast cells with Ct values close to or the same as canine lymphoma cells confirms that the heparin within the mast cells is not significantly inhibiting the binding and function of polymerase enzyme in this assay.

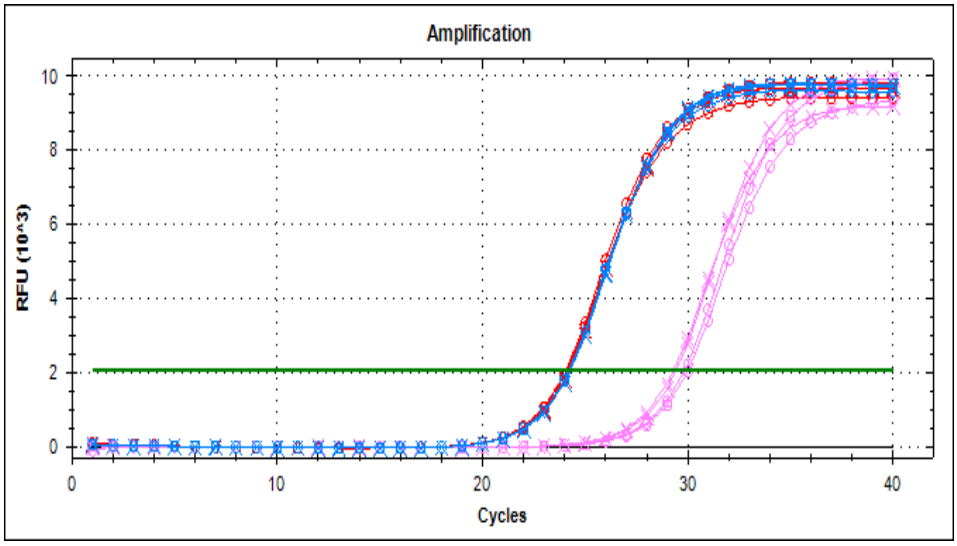

Figure 11. qPCR of one aspirated canine lymphoma (red) **and two mast cell tumors** (blue and pink)**.** O's represent RE1 single copy locus primers. X's represent "traditional" primers. Each sample was run in duplicate.

To verify that the SsoAdvanced SYBR Green Supermix (Bio-Rad) was able to amplify DNA extracted from FFPE MCTs without significant enzyme inhibition by formalin fixation, an aspirate of a non-Shar-Pei canine mast cell tumor was compared to two formalin-fixed paraffin embedded non-Shar-Pei MCTs in two separate experiments, using the "traditional" and MCR2 primers run in duplicate. As shown in **Figure 12** below, the Ct values for the aspirated MCT sample in green ranged from 23.05 to 23.24 cycles, the first FFPE MCT sample in blue ranged from 27.32 to 28.44 cycles, and the second MCT sample in red ranged from 33.46 to 36.42 cycles, all within the accepted range of less than 39 cycles, with similar results in both experiments (Bustin, 2009). The successful amplification of DNA from FFPE canine MCTs with Ct values close to aspirated MCTs confirms that FFPE samples are acceptable sources of DNA for use in qPCR assays.

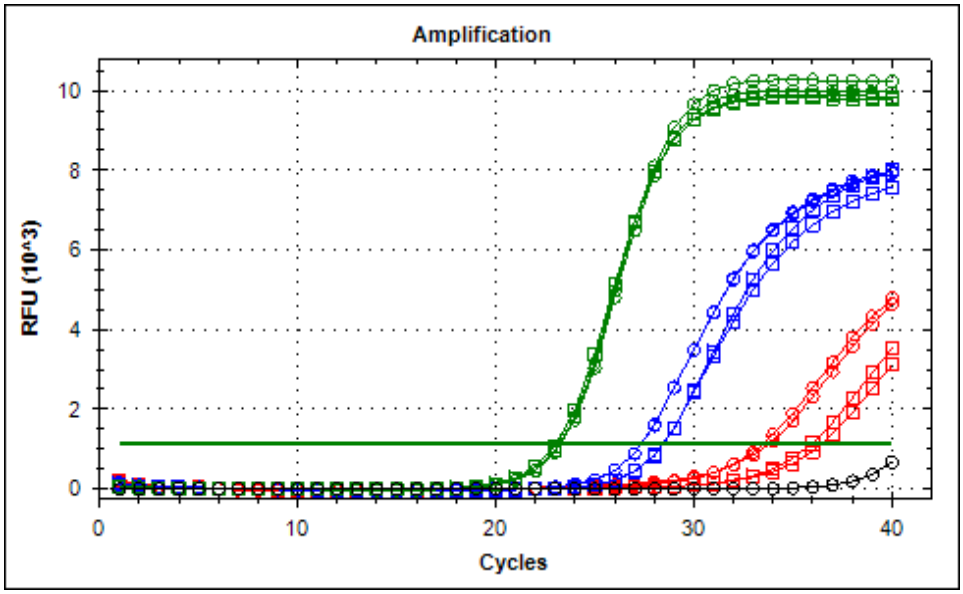

Figure 12. qPCR of one aspirated (green) **and two FFPE mast cell tumors** (blue and red)**.** O's represent "traditional" primers. Open boxes represent RE1 single copy locus primers. Each sample was performed in duplicate. The no template control is shown in black.

In all experiments during assay validation, and as shown in **Figure 13** below, each primer pair had distinct melt curves, confirming that each primer pair is specific, with no cross-amplification of non-target gene segments.

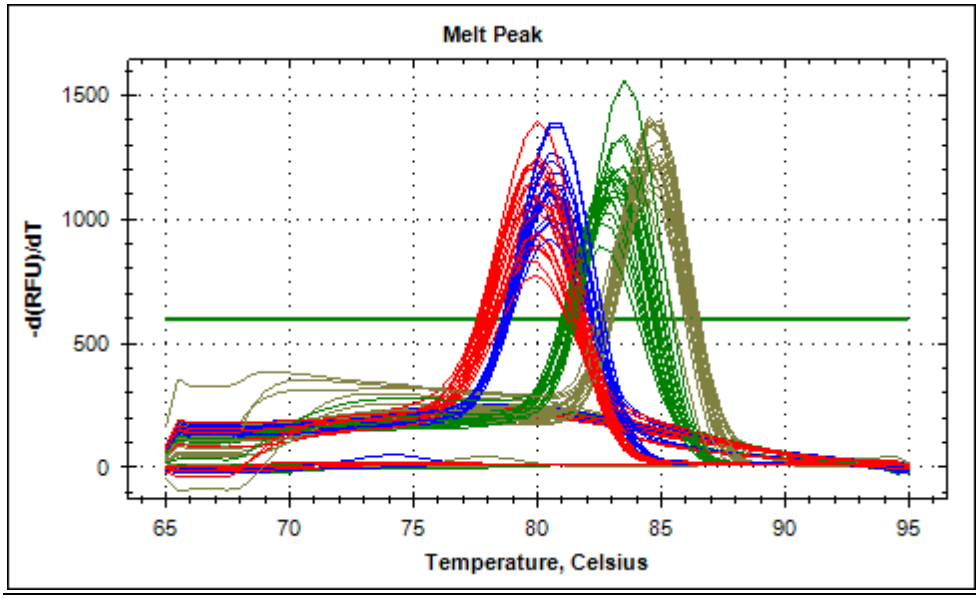

Figure 13. qPCR melt temperatures for 4 primer pairs (red = "meat-mouth", blue = "traditional", green = MC1R2, brown = RE1)

Additionally, serial dilution curves were performed to validate the use of the ddCt statistical method of relative gene copy number quantification by showing that the efficiencies of the primer pairs are close to 100% (+/- 10%) and similar enough to one another to maintain a constant relationship over the course of Ct values (25-35) relevant to the experiment (**Figures 14-17**).

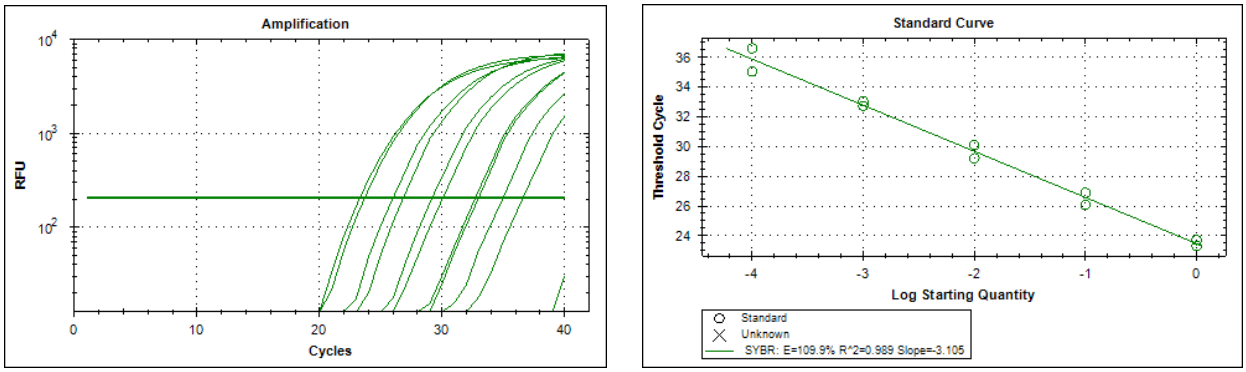

Figure 14. Dilution curve to determine "meat-mouth" primer efficiency (E=109.9%)

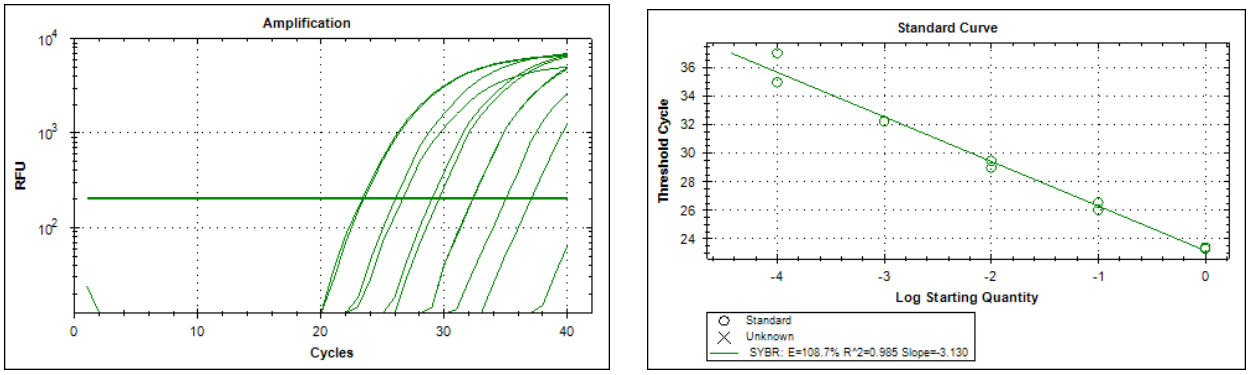

Figure 15. Dilution curve to determine "traditional" primer efficiency (E=108.7%)

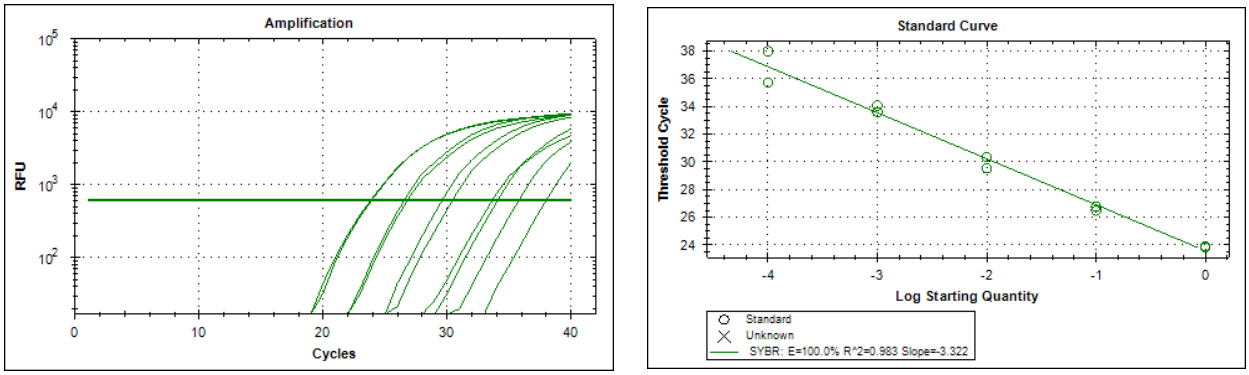

Figure 16. Dilution curve to determine MC1R2 primer efficiency (E=100.0%)

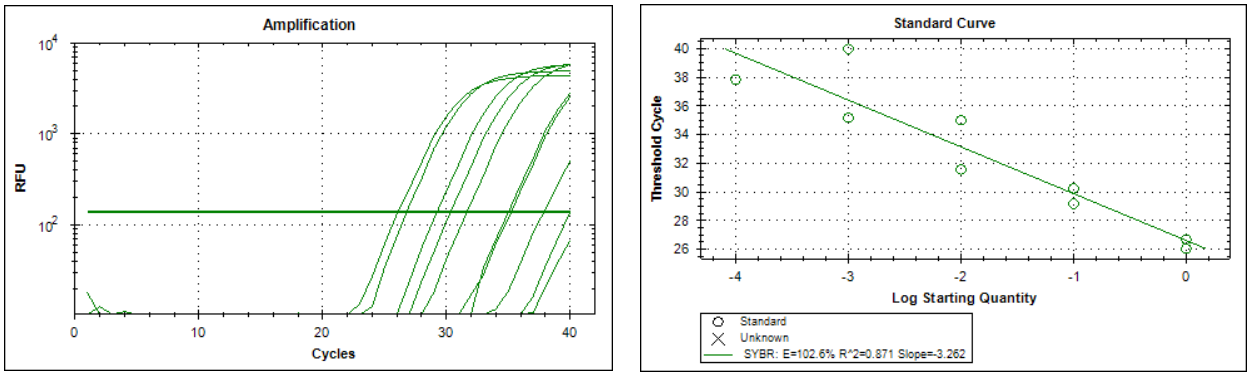

Figure 17. Dilution curve to determine RE1 primer efficiency (E=102.6%)

After validating the use of FFPE MCTs as sources of genomic DNA and the SsoAdvanced SYBR Green Supermix to amplify the DNA, we proceeded to use the assay to evaluate the relative copy numbers of our samples.

Gene duplications upstream of HAS2 are not restricted to neoplastic mast cells within Shar-Pei dogs

For our analysis of HAS2 copy number variation, we used DNA extracted from mast cell tumors. Although prior work has demonstrated that Shar-Pei contain HAS2 copy number variations in their germline, it was theoretically possible that the tumor itself could harbor duplications not found in the germline. Therefore qPCR was performed on a subset of 10 Shar-Pei MCTs and the corresponding tumor-adjacent skin, defined as tissue sections trimmed from the original biopsy specimen but submitted as separate tissue block and devoid of any identifiable tumor tissue. As shown in **Figure 18** below, the relative copy number determined for each section of tumor-adjacent skin is approximately equal to the relative copy number of the adjacent tumor. Also, the relative copy number for each sample is greater than 2, the copy number of a dog without any gene duplications. This suggests that the gene duplications are genome-wide within each Shar-Pei, and not a product of malignant transformation of mast cells.

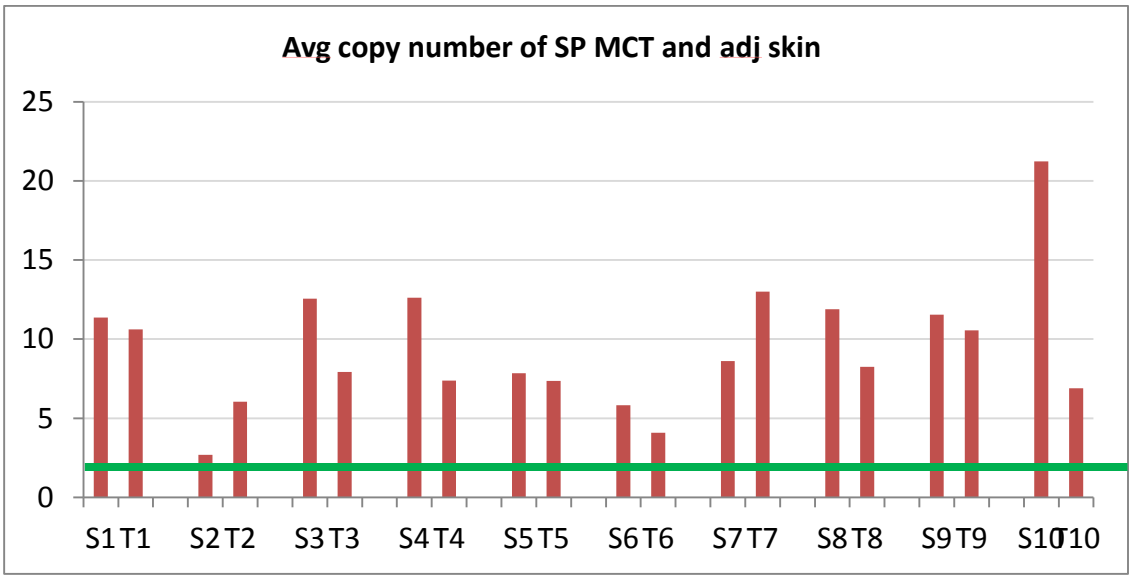

Figure 18. Comparison of average copy number between Shar-Pei MCTs (T1-10) **and tumor-adjacent skin** (S1-10). The green line represents a copy number of 2, representing no gene segment duplications.

Skin biopsies from Shar-Pei dogs have higher relative gene duplication copy numbers than skin from non-Shar-Pei dogs

qPCR was performed on 15 non-Shar-Pei and 75 Shar-Pei MCTs. The relative copy numbers of the meatmouth and traditional duplications for each sample were averaged for statistical analysis. The median copy number was 1.23 (range 0.46-3.13, outlier 12.985) for the non-Shar-Pei biopsies, and 11.71 (range 0.86-55.355) for the Shar-Pei biopsies (**Figure 19**). The Shar-Pei biopsies had significantly higher relative copy numbers than the non-Shar-Pei biopsies, as determined using a Wilcoxon rank sum test ($p<2.2x10^{-16}$), supporting the assumption that the gene duplications are unique to the Shar-Pei breed.

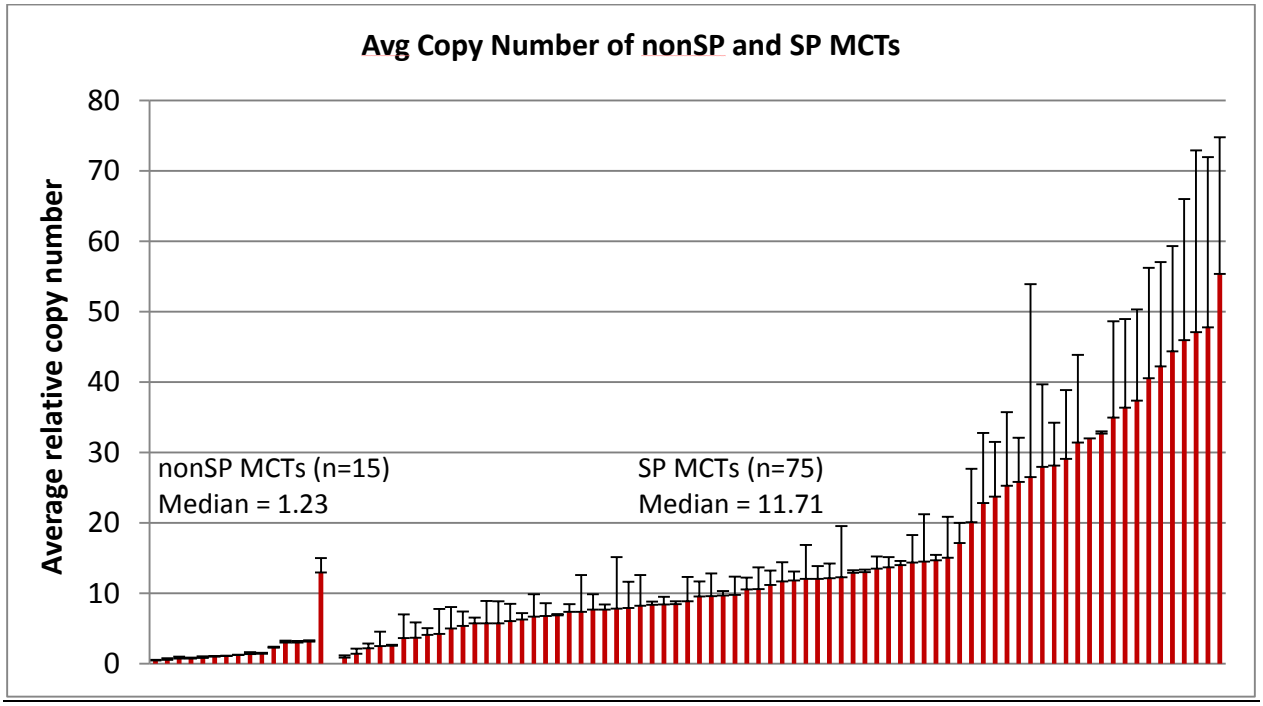

Figure 19. Comparison of average copy number between Shar-Pei and non-Shar-Pei MCTs

Grading and histologic evaluation of tumor features

Grade

Of the 149 Shar-Pei cutaneous mast cell tumors evaluated, 9 (6%) were Grade 1, 79 (53%) were Grade 2, and 61 (41%) were Grade 3 according to the Patnaik grading system (Patnaik, 1984). Using the two-tiered grading scheme (Kiupel, 2011), 60 (40%) were low-grade and 89 (60%) were high-grade.

Depth of invasion

Seven (4.7%) MCTs were confined to the superficial dermis (depth score 1), 28 (18.8%) extended into the deep dermis and limited subcutis (depth score 2), and 114 (76.5%) had significant invasion into the subcutis (depth score 3).

Cell pattern

Thirteen MCTs (8.7%) displayed a cell pattern consisting of rows or small groups of cells separated by mature collagen fibers of the dermis (cell pattern 1); 65 MCTs (43.6%) displayed moderate to high cellularity in large groups with thin fibrovascular stroma (cell pattern 2); and 71 MCTs (47.7%) displayed high cellularity in closely packed sheets with thick fibrovascular stroma that replaced most of subcutaneous and deep tissues (cell pattern 3).

Cellular differentiation

Forty-six MCTs (30.9%) displayed primarily round and monomorphic well-differentiated mast cells with ample cytoplasm, distinct cytoplasmic boundaries, and medium-sized granules (differentiation score 1); 44 MCTs (29.5%) displayed primarily round to ovoid cells, scattered spindle and giant cells, moderate anisocytosis and fine cytoplasmic granularity (differentiation score 2); and 59 MCTs (39.6%) displayed pleomorphic round, ovoid, or spindle cells, with giant cells and scattered multinucleated cells, marked anisocytosis, and indistinct or poorly granulated cytoplasm (differentiation score 3).

Nuclear typia

Eighteen MCTs (12.1%) displayed round and monomorphic nuclei with a condensed chromatin pattern (nuclear typia score 1); 73 MCTs (49%) displayed moderately pleomorphic, round to indented nuclei, with irregular chromatin, and a single prominent nucleolus (nuclear typia score 2); and 58 MCTs (38.9%) displayed pleomorphic nuclei with one or more large prominent nucleoli (nuclear typia score 3).

Karyomegaly

122 MCTs (81.9%) displayed minimal karyomegaly, with the nuclear diameter of less than 10% of neoplastic cells vary by at least 2-fold, and 27 (18.1%) displayed significant karyomegaly, with the nuclear diameter of at least 10% of neoplastic cells vary by at least 2-fold.

Mitotic index

The number of mitotic figures in ten 400x high-powered fields (mitotic index) ranged from 0 to 168, with 72 MCTs (48.3%) having a mitotic index less than 7, and 77 MCTs (51.7%) having a mitotic index greater than or equal to 7.

<u>Copy number is not significantly associated with degree of cutaneous mucinosis or depth of invasion, but is associated with grade, mitotic index, and microvessel density</u>

Of the 149 Shar-Pei MCT biopsies analyzed via light microscopy, 18 MCTs (12.1%) had 0% expansion of the dermis by pale basophilic stippled extracellular matrix (mucin score 0), 43 MCTs (28.9%) had 1-10% expansion of the dermis by mucin (mucin score 1), 37 MCTs (24.8%) had >10-20% expansion of the dermis by mucin (mucin score 2), and 51 MCTs (34.2%) had >20% expansion of the dermis by mucin (mucin score 3).

To evaluate the association of copy number and mucin score regardless of tumor presence, all MCT and MCT-free biopsies were grouped according to mucin score. The median copy number was 18.35 for mucin score 0 (n=10), 11.37 for mucin score 1 (n=31), 12.07 for mucin score 2 (n=21), and 10.55 for mucin score 3 (n=33). There was no significant difference in median copy number of Shar-Pei MCTs between the four mucin scores, as tested by the Kruskal-Wallis rank sum test (p=0.4734), and shown in **Figure 20** below. Similarly, no significant differences were found when the only Shar-Pei MCTs were compared (data not shown).

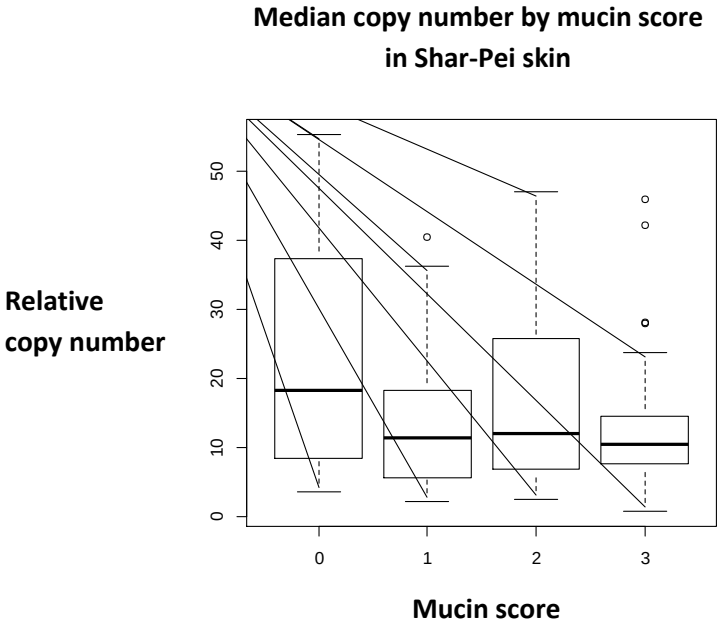

Figure 20. Comparison of median copy number by mucin score in Shar-Pei MCT and MCT-free skin combined by mucin score.

Grade and copy number were compared for 73 Shar-Pei MCT biopsies, as shown in **Figure 21** below. Grade III MCTs had significantly higher median copy number (13.1, n=30) than Grade I/II MCTs (9.54, n=43) under the Patnaik grading scheme, as determined by a Wilcoxon rank sum test

(p=0.007713). There was no significant difference between the median copy number of 9.54 for low-grade MCTs (n=33) and 11.95 for high-grade MCTs (n=40) under the Kiupel grading scheme (Wilcoxon rank sum, p=0.077).

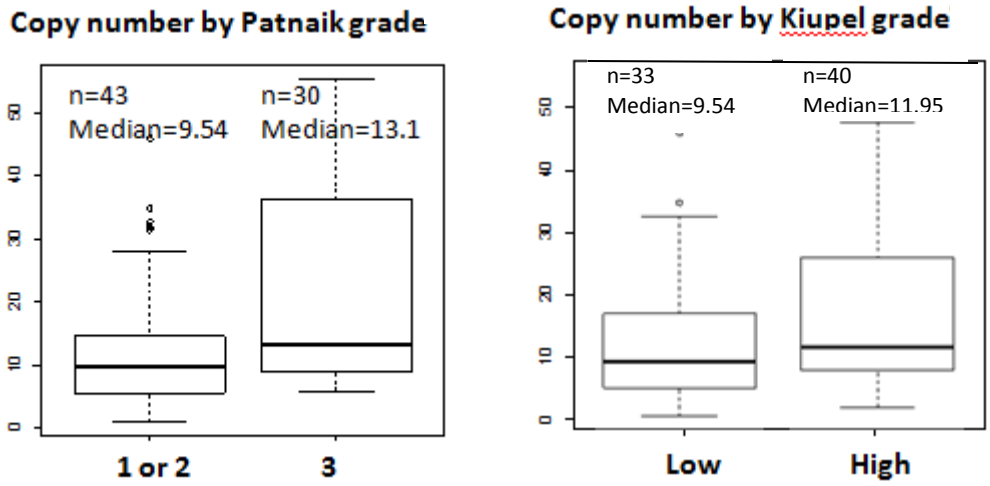

Figure 21. Average relative copy number by grade using Patnaik and Kiupel grading schemes

Copy number and depth of invasion were compared for 73 Shar-Pei MCT biopsies, as shown in **Figure 22** below. MCTs that were present only in the dermis had a median copy number of 12.04 (n=23), while those that invaded the subcutis had a median copy number of 10.86 (n=50), with no significant difference between groups (Wilcoxon rank sum, p=0.5175).

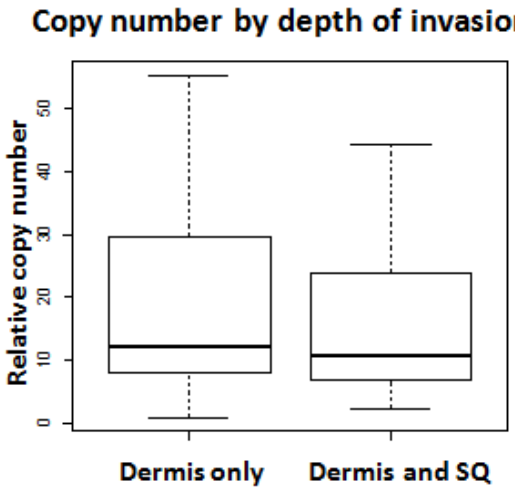

Figure 22. Average relative copy number by depth of invasion

Copy number and mitotic index were compared for 73 Shar-Pei MCT biopsies, as shown in **Figure 23** below. MCTs with a mitotic index greater than or equal to 7 had a significantly higher median copy number (12.17, n=35) than MCTs with a mitotic index less than 7 (9.615, n=38) as determined by a Wilcoxon rank sum test (p=0.02196).

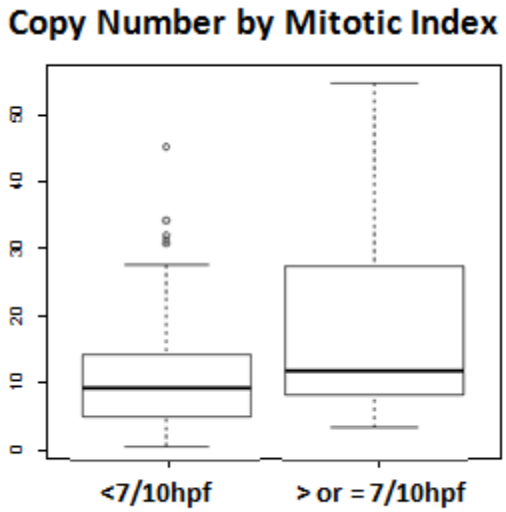

Figure 23. Average relative copy number by mitotic index

Copy number and microvessel density were compared for 73 Shar-Pei MCT biopsies, as shown in **Figure 24** below. A moderate positive correlation (R^2=0.1094) between copy number and microvessel density was found to be statistically significant (Pearson r correlation, p<0.05).

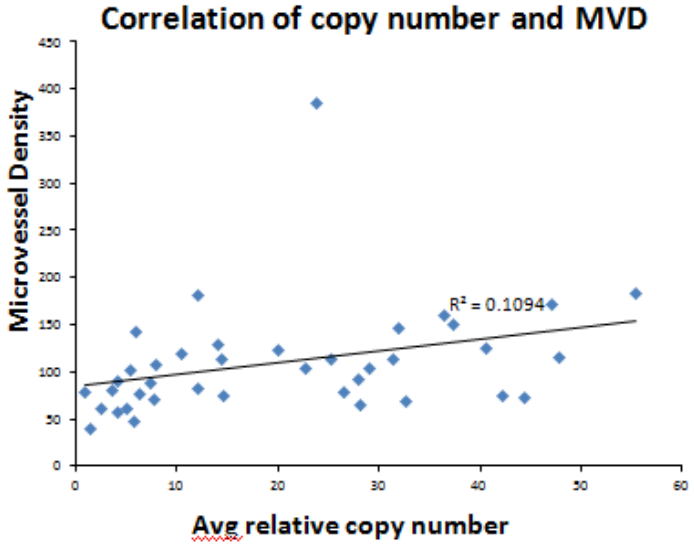

Figure 24. Correlation of average relative copy number and microvessel density

Degree of cutaneous mucinosis is not significantly associated with mitotic index, depth of invasion, histologic grade, or microvessel density in Shar-Pei MCTs

The degree of cutaneous mucinosis in 149 Shar-Pei MCTs was compared with mitotic index, depth of invasion, and histologic grade.

MCTs with a mucin score of 0 (n=18) had a median mitotic index of 11.5. MCTs with a mucin score of 1 (n=42) had a median mitotic index of 5. MCTs with a mucin score of 2 (n=37) had a median mitotic index of 5 MCTs with a mucin score of 3 (n=52) had a median mitotic index of 4.5. No significant difference was found between groups (Kruskal-Wallis rank sum test, p=0.6436).

Of MCTs with a mucin score of 0, 2 were restricted to the superficial dermis, 4 extended to the deep dermis, and 12 extended into the subcutis. MCTs with mucin scores of 2, 3, and 4 had similar distributions of depth of invasion (2, 8, 32; 1, 7, 29; and 5, 12, 35; respectively). No significant difference was found between groups (Fisher's exact test, p=0.7917).

Of MCTs with a mucin score of 0, 8 were Grade I or II and 10 were Grade III. MCTs with mucin scores of 2, 3, and 4 had similar distributions of grade (24, 18; 21, 16; and 35, 17; respectively). No significant difference was found between groups (Fisher's exact test, p=0.3641). Of MCTs with a mucin score of 0, 4 were low-grade and 14 were high-grade. MCTs with mucin scores of 2, 3, and 4 had similar distributions of grade (18, 24; 16, 21; and 22, 30; respectively). No significant difference was found between groups (Fisher's exact test, p=0.4276).

Determination of microvessel density by computer image analysis does not correlate with MVD determined by light microscopy in Shar-Pei MCTs

Microvessel density (MVD), reported as the total number of positive cell clusters in five 0.196 mm^2 (400x) microscope fields, was determined by light microscopy ("by hand") and using computer image analysis software for 46 Shar-Pei MCT biopsies. When comparing the MVD results between the two methods of evaluation using Pearson r correlation, there was found to be only a weak positive correlation between the methods, as shown below in **Figure 25** (R^2=0.062035, p=0.09517). This suggests that computer image analysis is not an accurate and reliable method of determining microvessel density in FFPE tumor biopsies.

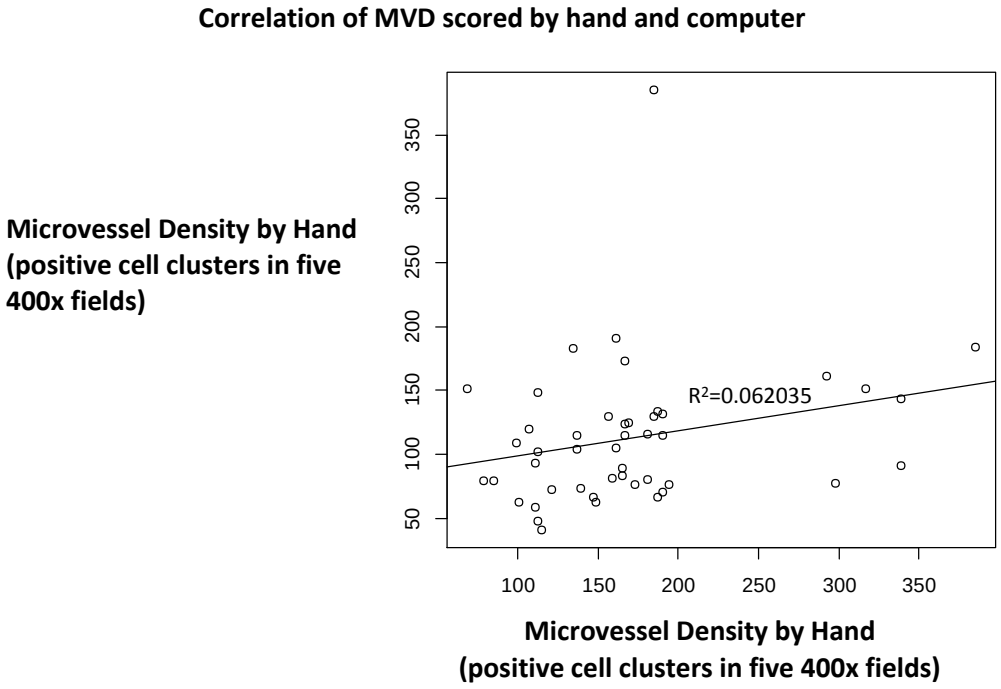

Figure 25. Correlation of microvessel density when scored by hand versus computer image analysis

Microvessel density is significantly associated with histologic grade, but not degree of cutaneous mucinosis in Shar-Pei MCTs

Microvessel density determined by hand in 46 Shar-Pei MCTs was compared with histologic grade and degree of cutaneous mucinosis.

21 MCTs were determined to be Grade I or II and low-grade by the two grading schemes, and had a mean MVD of 81 Factor VIII-positive cell clusters in five 400x hpf. 25 MCTs were determined to be Grade III and high-grade, and had a mean MVD of 116, which was significantly higher than the low-grade tumors, as determined by a Wilcoxon rank sum test (p=0.01154) and shown in **Figure 26** below.

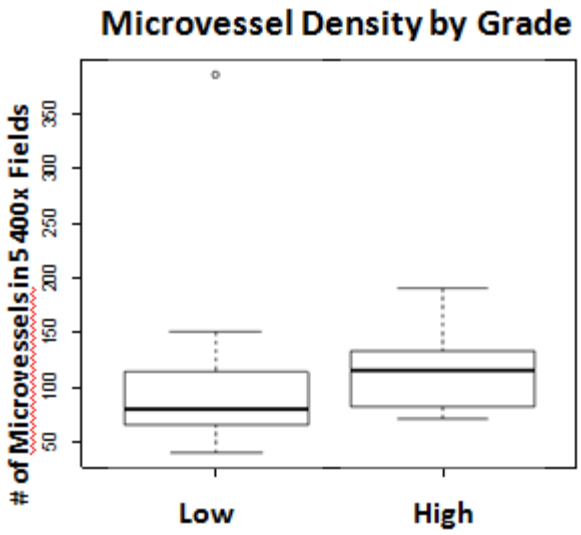

Figure 26. Median microvessel density compared with histologic grade in Shar-Pei MCTs

MCTs with a mucin score of 0 (n=7) had a median microvessel density of 116 when scored by hand, and 181 when scored using the ImageJ computer image analysis program. MCTs with a mucin score of 1 (n=14) had a median microvessel density of 115 by hand and 164 by computer. MCTs with a

mucin score of 2 (n=9) had a median microvessel density of 105 by hand and 161 by computer. MCTs with a mucin score of 3 (n=16) had a median microvessel density of 91 by hand and 156 by computer. No significant difference was found between groups, as shown in **Figure 27** below (Kruskal-Wallis chi-squared test, p=0.9174).

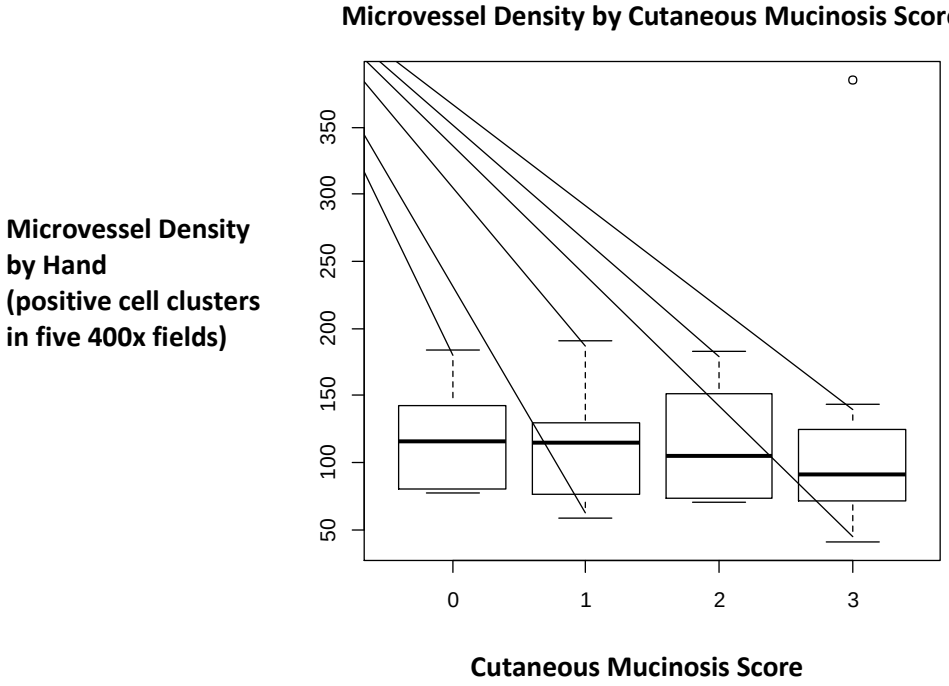

Figure 27. Microvessel density compared with cutaneous mucinosis score in Shar-Pei MCTs

DISCUSSION

The objective of this study was to evaluate the relationship between gene duplications upstream of the hyaluronic acid synthase 2 gene, cutaneous mucinosis, and features of mast cell tumor aggressiveness in Shar-Pei dogs. Biopsies of cutaneous MCTs from 149 Shar-Pei and 100 non-Shar-Pei were graded according to the Patnaik (1984) and Kiupel (2011) systems for canine cutaneous MCTs. Biopsies of the Shar-Pei MCTs were also evaluated for degree of cutaneous mucinosis, depth of invasion, and microvessel density (MVD). Shar-Pei and non-Shar-Pei MCTs were evaluated via qPCR for relative copy number of the gene duplication upstream of HAS2. The proportion of grade III tumors was significantly higher in Shar-Pei than the general canine population, but the average age at diagnosis was not significantly different between groups. Shar-Pei biopsies had significantly higher HAS2-associated gene segment duplications than non-Shar-Pei biopsies. Relative copy number was not significantly associated with the degree of cutaneous mucinosis. Grade III MCTs had a significantly higher copy number than grade I and II tumors using the Patnaik grading scheme, but there was no difference between copy numbers of high- and low-grade tumors in the Kiupel grading scheme. MCTs with a mitotic index > or = 7/10 hpf had a significantly higher copy number than those < 7/10hpf. Higher copy number was not associated with deeper invasion of MCTs, but did have a moderate positive correlation with microvessel density. MVD was also higher in high-grade MCTs than low-grade. Our data suggest a relationship between HAS2 gene duplications and features of MCT aggressiveness in Shar-Pei dogs.

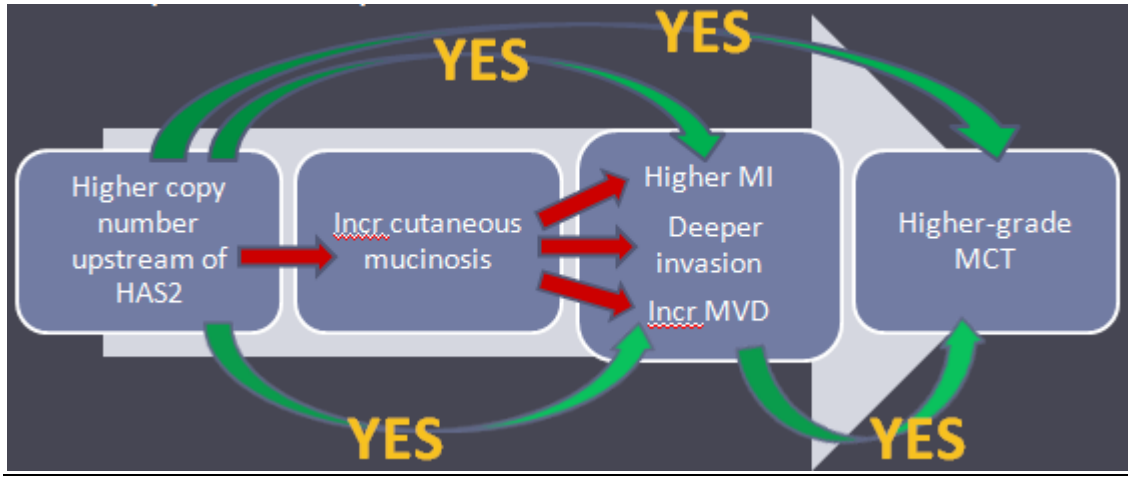

Figure 28. Summary of results according to proposed pathogenesis. Green arrows represent significant associations, and red arrows represent no significant association.

Exclusion of subcutaneous mast cell tumors

Subcutaneous mast cell tumors were defined as those tumors only found within the subcutaneous fat and deeper tissues, with no involvement of the dermis. These subcutaneous tumors were excluded from this study because they cannot be appropriately evaluated using the Patnaik grading scheme for canine cutaneous mast cell tumors (1984). Under that grading system, all subcutaneous mast cell tumors would be given a grade of II or III because of their location. Patnaik found that 47% of dogs with grade II MCTs, and 6% of dogs with grade III MCTs were still alive at 1500 days post-diagnosis. However, in a recent study of 306 subcutaneous canine MCTs, 84% of the dogs were alive at 1500 days post-diagnosis, supporting the idea that subcutaneous MCTs have a better prognosis than those arising in the dermis, and that the use of cutaneous MCT grading schemes are inappropriate for these cases (Thompson, 2011). Because of the variation in prognosis, inability to use current grading schemes, and the distance in location of development of these subcutaneous tumors as related to cutaneous mucinosis found in the dermis of Shar-Pei dogs, we chose to exclude subcutaneous MCTs from our study.

Role of age in MCT development in Shar-Pei dogs

Although it has been suggested in the literature that Shar-Pei get MCTs at a younger age than other breeds, there were relatively few biopsies included to represent Shar-Pei in these studies, and no statistical analyses were performed on the relationship between breed and age predispositions (Miller, 1995; Welle, 2008). In our comparison of MCTs from 97 Shar-Pei and 95 non-Shar-Pei dogs, the median age at time of biopsy was 8 years for both groups. Similarly, median ages across all breeds were reported to be 7.2-9 years in various reports (Kiupel, 2005; Scase, 2006; Simoes, 1994; Poggiani, 2012; Patnaik, 1984; Strefezzi, 2003). Since our findings are consistent with previous studies, it confirms that our random selection of 95 non-Shar-Pei dogs is representative of the greater canine population with respect to age. This is in contrast to the findings of Miller (1995), where 18 out of 802 cutaneous MCT biopsies were from Shar-Pei, and the median age for Shar-Pei was 5 years. The evaluation of 97 Shar-Pei over 10 years in our study, versus 18 Shar-Pei over 2 years in Miller's study, may have resulted in the differing findings, although both populations were from veterinary teaching hospitals. Additional studies are needed to confirm the role of Shar-Pei age in tumor development across tumor types. Perhaps an inherently unstable genome, such as that which leads to increased copy numbers upstream of HAS2, promotes oncogenesis in Shar-Pei dogs.

Inhibition of DNA amplification by formalin and heparin

Formalin is a commonly used tissue fixative for diagnostic purposes; however, it is not ideal for subsequent DNA extraction. Storage of tissues for greater than 1 week in formalin will destroy nucleic acids. Formalin fixation of shorter time periods, even diagnostically-relevant 12-24 hour periods, will result in extensive cross-linking of nucleic acids, resulting in fragmentation of DNA into 300-400bp fragments. Although short PCR products are desirable in qPCR protocols, fragmentation in the middle of

area of interest may affect qPCR results and skew the research findings (Lehmann, 2001). Modified DNA extraction protocols have been devised to try to minimize the effects of formalin fixation, but the extraction protocol used in this study was sufficient for reliable and consistent DNA extraction, evidenced by similar amplification profiles between fresh aspirated mast cell tumor samples and formalin-fixed MCT biopsies, as described in the results above.

Heparin, one of the major components of mast cell granules, can also inhibit DNA amplification during PCR reactions by binding to free and DNA-bound polymerase enzymes. Even low heparin concentrations can significantly inhibit the polymerase enzyme (Walter, 1967). The BIO-RAD SsoAdvanced SYBR Green Supermix used in this study contains a novel Sso7d fusion polymerase enzyme that is reported to be more resistance to PCR inhibitors and have higher processivity along the DNA template. During the validation phase of our study, we determined that DNA amplification from mast cell tumors was similar to that from lymphoma samples, demonstrating negligible inhibition of the polymerase enzyme by heparin.

Validation of qPCR assay with dilution curves

Because of the variable nature of submitted biopsy samples with respect to tissue dimensions and cellularity within the tissue block, the content of DNA in each extracted sample was unknown, and the DNA quantity was likely too low to be detected with fluorometric quantification. Six hundred to a few thousand nuclei are reported to be necessary for DNA quantification by this method (Rago, 1990; Downs, 1983). By diluting representative control samples and demonstrating linear standard curves showing consistent PCR efficiency (90-110%) over a range of Ct's relevant to the experiment (25-35), we can reliably compare samples with differing DNA concentrations (D'haene, 2010; Livak, 2001).

Calculation and variability of copy number data

Relative copy numbers of gene duplications are calculated values, not measured (Livak, 2001), therefore the results calculated will not always be in precise multiples of one or two copies. Additionally, sister chromatids of canine chromosome 13, within the same and neighboring cells, may have different copy numbers due to the nature of copy number variation via nonallelic homologous recombination and nonhomologus end joining during mitosis and meiosis (Alvarez, 2012).

For the same reasons, relative copy numbers varied slightly between the SP MCTs and adjacent skin in our study. Additionally, although the gene duplications are germline, and not somatic, mast cells and adjacent epithelial and mesenchymal cells within the surrounding skin come from different cell lines, and their respective stem cells may have had more or fewer meiotic or mitotic events resulting in copy number variation.

Use of mitotic index as an indication of cell proliferation

While higher copy number was significantly associated with a mitotic index greater than 7 in our study, a strong linear relationship between these continuous variables was not found. Mitotic index is the most widely used indicator of cell proliferation in canine cutaneous mast cell tumors, but the prognostic significance of other proliferation indices has been examined.

Nucleolar organizer regions that bind silver nitrate stains (AgNORs) are the sites of rRNA transcription in all nuclei, and are thus indicators of cell replication. MCTs with greater than or equal to 4 AgNORs per cell have a worse prognosis than tumors with less than 4 AgNORs per cell, with median survival times of 17 and greater than 50 weeks, respectively (Bostock, 1989). In the same study, AgNORs were found to be a better predictor of tumor-related death than mitotic index alone, which was

corroborated by Simoes and colleagues in a comparison of AgNOR counts, PCNA, mitotic index, and histologic grade (1994).

Proliferating cell nuclear antigen (PCNA) is a protein labeled via IHC that is associated with the delta subunit of the polymerase enzyme, enhancing processivity, and is required for DNA synthesis (Simoes, 1994). PCNA is expressed in the S and M phases of the cell cycle (Scase, 2006). PCNA is a significant predictor of MCT recurrence and metastasis and was found to be a better predictor of recurrence than mitotic index (Simoes, 1994).

Ki-67 is a large protein that is a key player in the cell cycle, with highly regulated location and expression during the cell cycle, but its function is poorly understood. The Ki-67 value for a tumor is reported as the percentage of nuclei positively stained with the MIB-1 monoclonal antibody. The Ki-67 score is significantly associated with survival time across all mast cell tumors, with the added benefit of helping to predict which grade II MCTs are more likely to recur or metastasize (Scase, 2006).

Therefore, while mitotic index alone has been shown to be a significant prognostic indicator in multiple studies of canine cutaneous MCTs (Simoes, 1994; Preziosi, 2004; Romansik, 2007; Preziosi, 2007; Elston, 2009), a more accurate relationship between HAS2 copy number and tumor cell proliferation and prognosis may be possible with subsequent evaluation of AgNORs, PCNA, or Ki-67.

Evaluation of peripheral versus intratumoral mucinosis

Canine cutaneous mast cell tumors are often described as having peripheral or intratumoral expansion by mucinous edema (Welle, 2008; Zanna, 2009). Typically, human and canine tumor-associated mucinosis is thought to be a result of direct production of HA by neoplastic cells, or a result of fibroblast stimulation by neoplastic cells, resulting in upregulation of HAS2 gene expression and

increased hyaluronan production after initiation of the tumor (Knudson, 1996; Itano, 2011; Pasonen-Seppanen, 2012; Saito, 2013; Mukaratirwa and Chimonyo, 2004; Mukaratirwa and van Ederen, 2004; Ropponen, 2008; Serra, 2004). One of the goals of our experiment was to determine if the degree of cutaneous mucinosis inherent in each Shar-Pei predisposes it to the development of cutaneous mast cell tumors. Therefore, we chose to evaluate skin as far from the tumor as possible, but still within the original biopsy, to represent the baseline cutaneous mucinosis of the dog prior to the development of the mast cell tumor. If we had evaluated the amount of mucin within or adjacent to the mast cell tumor, it would have been unclear whether the tumor or mucinosis came first.

Cutaneous mucinosis in Shar-Pei dogs is typically more pronounced on the head, neck, and distal extremities (Zanna, 2008; Lopez, 1999). The locations of MCTs used in our study were not evaluated, and it would have been interesting to determine if MCTs in Shar-Pei are more likely to occur in these locations than in other breeds. This relationship may also support an association between cutaneous mucinosis and MCT development. Accordingly, it may have been more informative to collect biopsy samples from the areas of most pronounced mucinosis when comparing copy numbers to extent of dermal mucin; however, if the development of MCTs is affected by the mucin in the pre-existing microenvironment, then evaluation of mucin in the skin closest to the tumor, as performed in this study, is most appropriate. Also, since this is a retrospective study, biopsy site could not be controlled, nor additional biopsies recommended for dogs included in the study. In a prospective study, biopsy of the corresponding but contralateral skin (left hock if tumor on right hock), may be the most accurate representation of mucinosis at the tumor site without being influenced by the effects of the tumor itself.

Use of Factor VIII-related antigen to measure microvessel density

Intratumoral microvessel density has been shown to be a significant prognostic indicator in numerous human and canine tumors, including canine cutaneous mast cell tumors (Preziosi, 2004; Poggiani, 2012; Passantino, 2008; Luong, 2006; Weidner, 1991; Lavalle, 2009; Barbosa, 2013). The most commonly used immunohistochemical marker of vascular endothelium in canine studies is factor VIII-related antigen, also known as von Willebrand's factor. Factor VIII-related antigen is a protein important in platelet adhesion at sites of vascular injury, and is stored in Weibel-Palade bodies in the cytoplasm of endothelial cells and megakaryocytes (Jennings, 2012; Pusztaszeri, 2006).

Other immunohistochemical markers used in canine, feline, and human studies include CD31, CD34, CD105 with caldesmon, and Fli-1, with multiple studies comparing the staining qualities and diagnostic and prognostic usefulness of these markers (Clemente, 2010; Jennings, 2012; Luong, 2006; Hansen, 2010; Sleeckx, 2013; Pusztaszeri, 2006). CD31, also known as platelet-endothelial cell adhesion molecule-1 (PECAM-1), is a transmembrane glycoprotein present on the surface of platelets, megakaryocytes, endothelial cells, and leukocytes, and it functions to facilitate adhesion and transmigration of leukocytes (Jennings, 2012; Pusztaszeri, 2006). CD34 is a transmembrane glycoprotein with unknown function present on endothelial cells, hematopoietic stem cells, nerves, hair follicles, muscle bundles, sweat glands, and mesenchymal neoplasms (Jennings, 2012; Pusztaszeri, 2006). Immature vessels are identified as CD105 positive (a co-receptor for transforming growth factor beta found on blood and lymphatic endothelium, also known as endoglin) and caldesmon negative (a marker for smooth muscle) (Hansen, 2010). Fli-1 (Friend leukemia virus integration-1) is a nuclear transcription factor expressed in endothelium and hematopoietic cells, with consistently high vascular immunoreactivity in normal human parenchymal tissue (Pusztaszeri, 2006). To the best of our

knowledge, CD105 and Fli-1 have not been validated in peer-reviewed publications for used in FFPE canine tissue.

Reports of the relative specificity and level of background staining of factor VIII-related antigen as compared to CD31 and CD34 in canine and feline tissues is variable (Clemente, 2010; Jennings, 2012; Luong, 2006; Sleeckx, 2013), but factor VIII-related antigen is more often significantly associated with metastasis, tumor-related death, survival time, grade, necrosis, mitotic index, and depth of invasion in canine neoplasms (Luong, 2006; Barbosa, 2013; Preziosi, 2004; Poggiani, 2012; Passantino, 2008) than CD31 and CD34 (Lavalle, 2009; Luong, 2006). This may be due in part to fewer studies being performed with CD31 and CD34 on canine FFPE tissues.

None of these markers are specific to endothelial cells, and all stain blood as well as lymphatic vascular endothelium (Pusztaszeri, 2006). The distinction between blood and lymphatic vascular endothelium may not be relevant in the study of tumor angiogenesis, as tumors grow new blood and lymphatic vessels during expansion, and both are potential routes of metastasis. Due to the extensive evaluation in the literature, and the frequency and proficiency of use of factor VIII-related antigen immunohistochemistry in our histology laboratory for routine diagnostic cases, factor VIII-related antigen was chosen as the marker of choice for endothelial cells in our evaluation of microvessel density.

Limitations

Multiple qPCR control samples

The inclusion of a reference sample is important for any PCR assay, but essential for copy number variation assays, where the finals results are reported as a copy number relative to a reference

sample with a known copy number (D'haene, 2010). In our study, 15 FFPE non-Shar-Pei MCT biopsies were used as reference (control) samples. Ideally we would have used DNA from only one reference sample for all assays performed. As control samples were sourced from Colorado State University Clinical Immunology Laboratory submissions, it was not possible to acquire enough DNA from one sample to perform all assays. Submission forms were reviewed to determine the breed of each control sample, excluding Shar-Pei and Shar-Pei mixes. All control samples were evaluated via qPCR assays with multiple other controls to allow comparison of relative copy number results between samples in light of the control used on each plate.

In a previous study identifying the gene duplications upstream of HAS2 (Olsson, 2011), none of the 73 non-Shar-Pei control dogs were found to have elevated copy numbers. It was concluded that these gene duplications are unique to the Shar-Pei breed; therefore, non-Shar-Pei biopsies in our study were expected to have a relative copy number of 2. The relative copy number of 14 of our 15 control samples ranged from 0.46 to 3.13, but one control had a relative copy number of 12.985. This sample was from a Shetland sheepdog, and the cause for this outlier could not be determined. Perhaps there was a spontaneous mutation of a gene segment overlapping our region of interest, or the breed was erroneously reported on the submission form. Having a control sample with higher than expected results may have caused artificially low relative copy numbers in the samples run with that control. Therefore, while we expected all control dogs to have copy numbers of around 2, pooling all of our control DNA would have resulted in more precise results across our test samples. This method modification will be performed in future studies.

Limitations of computer image analysis with ImageJ

Evaluation of tumor microvessel density has been performed in numerous studies of canine and human neoplasms, using a variety of methods (Hansen, 2004; Fox, 1995; Hansen, 1998). Multiple comparisons of computer image analysis with more traditional counting of vessels by pathologists have concluded that computerized counts are reliable, rapid, and correlate well with traditional hand counts (Wild, 2000; Fox, 1995). An additional benefit to computer analysis is the ability to calculate the percent area of the image that is stained by vascular markers, estimating the vascular volume within the tissue section. In contrast, other studies have found no correlation between hand counts and computer analysis, with hand counts having more prognostic significance than computer analysis (Kohlberger, 1996).

Multiple computer image analysis programs are available for this analysis, including Cytometrica (Preziosi, 2004), Leica QWin (Poggiani, 2012), Quantimet 500 (Passantino, 2008), and the free open-source program ImageJ (NIH, Bethesda, Maryland, USA) used in our study. In this study, computerized counts of microvessel density, reported as factor VIII-related antigen immunopositive cells clusters in five 0.196 mm^2 400x fields, did not correlate well with traditional hand counts ($p=0.09517$), with computerized counts often overestimating the number of vessels. Hand counting is thought to be a more accurate method of vessel identification, because classification of a vessel relies on tissue architecture and educated interpretation of IHC staining that is not possible with current computer programs.

Computer image analysis was conducted in this study using a macro to ensure consistent color and size thresholding and subsequent rapid evaluation of each image. As demonstrated in the Materials and Methods section above (Figure X, a-c), size thresholding was necessary to remove non-endothelial nuclei from the image, but consequently resulted in loss of detail of the small arteriole in the top center

of the image. Because the positive staining of endothelial cells did not form a continuous ring with a lumen, the image was interpreted as two small immunopositive cells, instead of one larger arteriole with a lumen. This altered interpretation thus created an error in vessel count as well as the percentage of the image area that corresponded to vascular endothelium and lumina. Setting thresholds for each individual image would have more accurately represented the vascularity of each tissue section; however, the benefit of reduction in time necessary to evaluate the captured images by using the macro for consistent image processing would have been lost. Therefore, computer image analysis using ImageJ was not determined to be a simultaneously accurate and rapid method of determining microvessel density.

Shar-Pei phenotype status unknown

In the United States, “meat-mouth” Shar-Pei, with their wrinkly skin, are more popular than the traditional smooth-coated Shar-Pei. With the retrospective nature of this study, the phenotype of the dogs included could not be determined, as this is not a standard feature described in medical records. Therefore, we could not predict what gene duplications we would see in each case. We were also unaware of which dogs had current or past episodes of Shar-Pei fever. An association between skin phenotype, history of Shar-Pei fever, and tumor grade would have strengthened our study and supported our hypothesis of a relationship between HA and tumor grade.

Future directions

More sensitive detection of degree of cutaneous mucinosis

Although we have shown that Shar-Pei develop higher-grade MCTs than the general canine population, and that gene duplications upstream of HAS2 were significantly associated with tumor grade, mitotic index, and microvessel density, we were not able to determine a significant association with the gene duplications and the degree of cutaneous mucinosis within the skin flanking the mast cell tumors. Additionally, we did not find a relationship between degree of cutaneous mucinosis and mitotic index, depth of invasion, histologic grade, or microvessel density.

In this study, cutaneous mucinosis was scored via light microscopy by the degree of separation of adjacent collagen bundles by extracellular basophilic stippling interpreted as mucin. The major component of dermal mucin in dogs is hyaluronan. Therefore, this novel scoring system is a relatively subjective measure of dermal HA levels, and may result in variation in interpretation.

A more accurate method of determining tissue levels of HA in our biopsies was attempted in a subset of 50 tumors. Previous studies have successfully used histochemical staining with biotinylated hyaluronan binding complex (bHABC; Seikagaku Kogyo Co., Tokyo, Japan) to identify HA in FFPE canine tissues (Mukaratirwa and van Ederen, 2004; Mukaratirwa and Chimonyo, 2004; Zanna, 2008; Zanna, 2009). However, to the best of our knowledge, that reagent is no longer commercially available and no commercial preparations of anti-hyaluronan antibody validated for use in canine FFPE tissues are available. An anti-hyaluronic acid antibody is available from Abcam (ab53842; Cambridge, Massachusetts, USA), that has been successfully tested in FFPE mouse, pig, chicken, and human tissues. In our multiple attempts to test the antibody's performance in canine tissue, no staining of positive control brain tissue was seen. Perhaps, with continued protocol modifications, a system may be devised for successful use in canine tissues.

Another potential method of semiquantification of hyaluronan in canine tissues is to stain FFPE sections with 1% alcian blue (pH a2.6) and periodic acid-Schiff histochemical stains, which together target acid glycosaminoglycans. Serial tissue sections are stained similarly, with a pretreatment of bacterial hyaluronidase, to confirm the detection and extent of hyaluronan present (Doliger, 1995; Zanna, 2008). In a study of cutaneous mucinosis in Shar-Pei dogs, the dermal mucin was found to bind strongly to both the alcian blue and the BHABC, suggesting their similar usefulness as markers of HA in canine skin (Zanna, 2008), and an important next step in our investigation.

Prognostic value of copy number in Shar-Pei MCTs

To provide the most useful data to clinicians and pathologists regarding the utility of determining HAS2 gene duplication copy numbers and degree of cutaneous mucinosis in their Shar-Pei patients, additional follow-up information will need to be acquired from referring veterinarians and owners about the cases used in this study, with consideration for proper methods of determining prognostic significance in veterinary oncology (Webster, 2011). Information to be collected in future analyses includes date of diagnosis, clinical stage at diagnosis, treatments performed, date of local recurrence or metastasis, history of cyclic fever or renal disease, and date and cause of death.

In our study, copy number was only significantly associated with one of two prognostically significant grading schemes for canine cutaneous MCTs. The main difference between the grading schemes is the use of quantitative cut-off values for numbers of mitotic figures, bi- and multi-nucleated cells, and karyomegaly within the neoplastic cell population. As such, 10 of the tumors for which copy number was determined were given a grade of 2 using the Patnaik scheme and a high grade using the Kiupel scheme. This difference in classification may be relevant to our study if the gene duplications are contributing to the higher mitotic index and karyomegaly, as we suspect they are.

Microvessel density has already shown prognostic significance with regard to survival time (Preziosi, 2004) and tumor-associated death (Barbosa, 2013), but not cancer free interval (Preziosi, 2004) in canine cutaneous mast cell tumors. Additionally, evaluation of the presence of metastatic disease at the time of biopsy or time to metastasis may further support a relationship between microvessel density and prognosis, with the prediction that tumors with a high microvessel density are more likely to metastasize earlier in the course of disease. Evaluation of these parameters in our Shar-Pei MCT cases may greatly aid in treatment decisions and give owners a more accurate prediction of the course of disease their pets.

Effect of gene duplications on angiogenesis

Future studies to prospectively test the effects of hyaluronan on angiogenesis, tumor cell motility and invasion, and tumor cell proliferation are best performed in the controlled setting of in vitro assays using cell cultures. Many canine mast cell tumor cell lines have been established (Ishiguro, 2001; Lin, 2009; Ohmori, 2008; Lazarus, 1986; Pennington, 1992; DeVinney, 1990), but none are reported to be derived from Shar-Pei dogs. Therefore, the establishment of one or multiple new cell lines of neoplastic mast cells from Shar-Pei dogs may need to be established, by such methods as described by Lin (2009) and Ohmori (2008).

The proposed pathogenesis for the promotion of angiogenesis in Shar-Pei MCTs is that dogs with higher copy number will have greater upregulation of HAS2 in the dermal fibroblasts and in the neoplastic mast cells, resulting in increased production of HA and stimulating angiogenesis, as compared to dogs with lower copy number. Dermal fibroblasts cultured from Shar-Pei dogs with higher copy numbers have been shown to have increased HAS2 expression (Olsson, 2011), and Shar-Pei fibroblasts with increased mRNA expression of HAS2 produce more HA than non-Shar-Pei canine fibroblasts (Zanna,

2009; Docampo, 2011). Hyaluronan has also been shown to be proangiogenic in many studies reviewed by Itano (2011).

In our study, we were able to show a moderate positive correlation between copy number and microvessel density in Shar-Pei MCTs. To explore this mechanism in more detail, in vitro experiments are recommended to allow for more control over the microenvironment. An interesting application of microfluidics can be employed to answer the question: "Do cultured fibroblasts from Shar-Pei dogs with higher HAS2 copy numbers stimulate more prolific angiogenesis than fibroblasts with lower copy numbers?"

In 2012, Kim and colleagues described a new technique for studying cell-cell interactions in an in vitro microfluidic cell culture model using cell encapsulation in alginate beads (**shown in Figure 29 below**). In brief, as applied to our study question above, a canine (or human) microvascular endothelial cell culture would be seeded into the central channel of a three-channel polydimethylsiloxane gel to form a monolayer. Cultured Shar-Pei dermal fibroblasts with known copy numbers (perhaps those used in Olsson's study in 2011) would be encapsulated in alginate beads and seeded into the first channel, with empty beads seeded into the third channel. A collagen scaffold separates each channel, and the size and number of endothelial buds with lumen-like structures into the collagen scaffold would be quantified using immunofluorescent rhodamine-phalloidin staining of actin filaments and DAPI staining of nuclei, visualized with confocal microscopy. The experiment could be repeated with the use of neoplastic mast cells in the alginate beads instead of the dermal fibroblasts to evaluate the effect of the two cell types on angiogenesis in each patient.

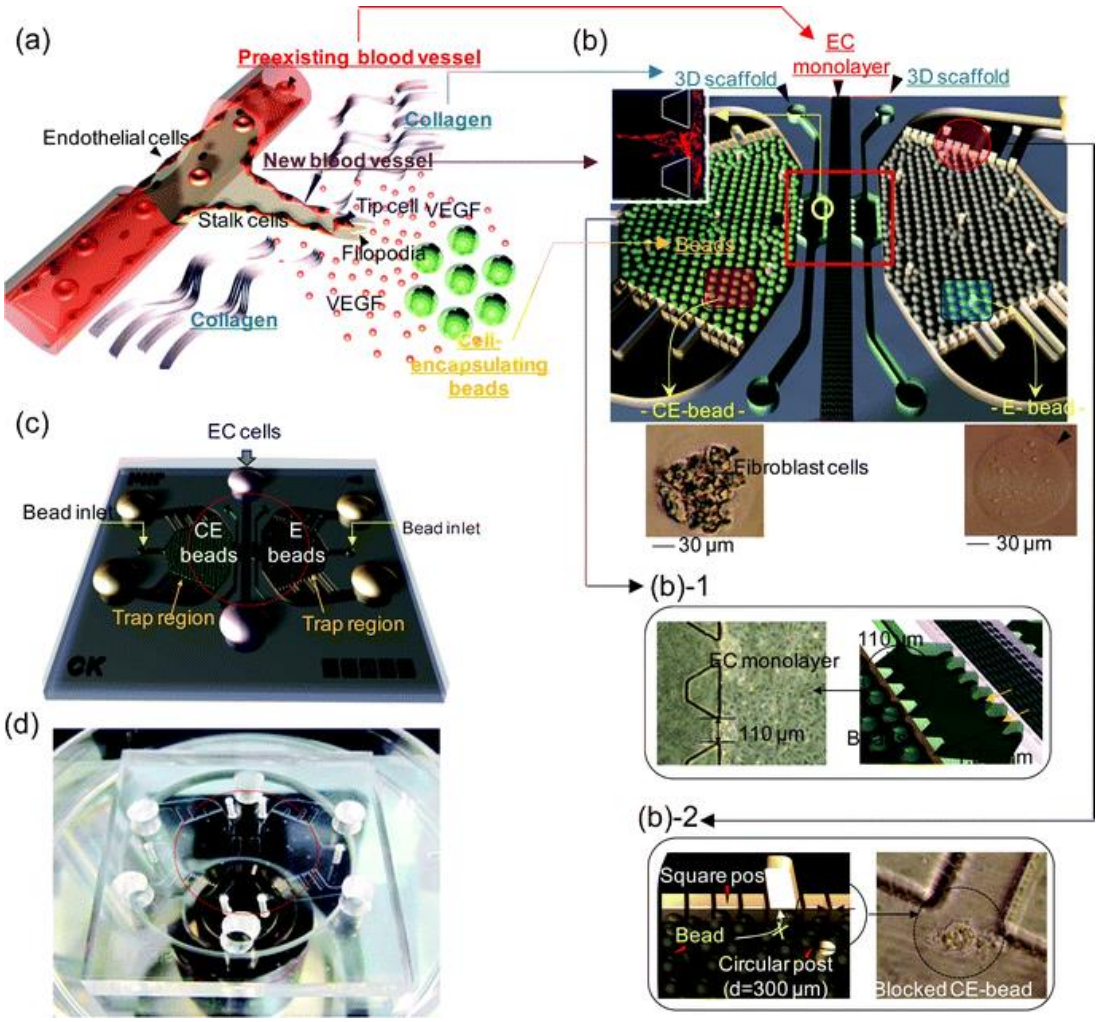

Figure 29. (from Kim, 2012) ***In vivo* angiogenesis application and microfluidic assay**. (a) Potential *in vivo* angiogenesis application in which cell-encapsulating beads secrete growth factors to elicit an angiogenic response. (b) Schematic view of the angiogenesis model for cell encapsulation-based cellular therapy. The angiogenesis-on-a-chip system was composed of three basic units: hydrogel scaffolds to mimic the extracellular matrix (ECM), a central microfluidic channel for forming an endothelial cell (EC) monolayer, and bead-trap regions for attracting sprouting angiogenesis. (b)-1: The width of the collagen gel region is 1.25 mm; each gel channel is partitioned using a series of regularly spaced posts (110 μm apart), (b)-2: Circular-shaped posts (diameter = 300 μm) prevent the upper side of the trap region from sticking to the cover slip; square-shaped posts (distance between posts = 50 μm) are positioned to prevent beads from escaping the bead-trap region. (c) Schematic view of the microfluidic assay. (d) Photograph of the complete system.

Effect of gene duplications on tumor cell motility and invasion

The proposed pathogenesis for the promotion of tumor cell invasion in Shar-Pei MCTs is that dogs with higher copy number will have greater upregulation of HAS2 in the dermal fibroblasts and in the neoplastic mast cells, resulting in increased production of HA. This increased HA in the extracellular matrix will make it easier for neoplastic cells to migrate through the dermis by attracting water into the extracellular matrix and separating adjacent collagen fibers. We predicted that deeper invasion of the Shar-Pei MCTs in our study into the dermis and subcutis would be associated with higher copy numbers; however, there was no statistical difference between median copy number in tumors that were restricted to the dermis versus those that extended from the dermis into the subcutis and deeper tissues.

Depth of invasion of the tumor was chosen as a histologic indicator of the ability of the neoplastic mast cells in each case to migrate through the dermal extracellular matrix. However, given the retrospective nature of this study, many factors may have affected the depth of tumor invasion at the time of biopsy, including owner decisions regarding the appropriate time for surgery within the clinical course of disease. To investigate this potential relationship between MCT migration, invasiveness, and copy number, in vitro assays would be preferred. Hyaluronan is known to induce expansion of the extracellular matrix because of tissue hydration due to increased osmotic pressure (Knudson, 1996). Therefore, the research question at hand is: “Do cultured dermal fibroblasts from Shar-Pei dogs with higher copy numbers allow more rapid migration of neoplastic mast cells through the collagen-rich dermis?” To investigate this question, cultured dermal fibroblasts of known copy number from Shar-Pei dogs would be co-cultured with a single established line of canine cutaneous neoplastic mast cells, with a collagen scaffold separating the two chambers, similar to that described above to test angiogenesis. We predict that neoplastic mast cells would be able to migrate through the collagen

scaffold more rapidly and in greater numbers when co-cultured with dermal fibroblasts of a higher copy number due to expansion of the collagen matrix and separation of collagen fibrils.

If the invasive potential of the tumor is determined by features of the neoplastic mast cells themselves, such as tumor cell production of HA or cell surface expression of CD44, and not a feature of the extracellular matrix, additional studies are needed. Migration through the dermis can be achieved by degradation and remodeling of the interstitium, as seen with mesenchymal-type migration of neoplastic cells, or by amoeboid migration between collagen fibrils without proteolysis (Wolf, 2003). To evaluate the differential ability of Shar-Pei MCTs to migrate through the dermal extracellular matrix, cultured Shar-Pei MCT cells of known copy number would be incorporated into 3D collagen lattices, then monitored with time-lapse video microscopy to determine the speed of migration and morphology of migrating MCT cells (Wolf, 2003). We predict that MCTs with higher copy number would migrate through the collagen matrix more rapidly than those with lower copy number or controls.

While migration through the dermis is necessary for neoplastic mast cells to approach nearby mature vessels, penetration through the vascular basement membrane is necessary for intravasation and metastatic potential. Metastatic potential was not evaluated in the current study, but future evaluation would include an in vitro assay using a Boyden chamber to determine the ability of neoplastic MCTs of known copy number from Shar-Pei dogs to migrate through a matrigel barrier and porous filter into a chemoattractant medium, as described by Albini in 1987, and shown in **Figure 30** below. The potential mechanism for increased invasiveness of neoplastic mast cells with high copy numbers is unclear and would require more specific study of the production of collagenases, trytpase, and chymase in these neoplastic cells (Liu, 2011). Shar-Pei with cutaneous mucinosis have been shown to have a higher percentage of tryptase-only-containing mast cells (T-MC) and a lower percentage of both chymase-only- (C-MC) and chymase-and-tryptase-containing (TC-MC) mast cells in the skin than control

dogs; however, further studies are needed to understand the differential role in degradation of basement membrane by these three cell types (Welle, 1999).

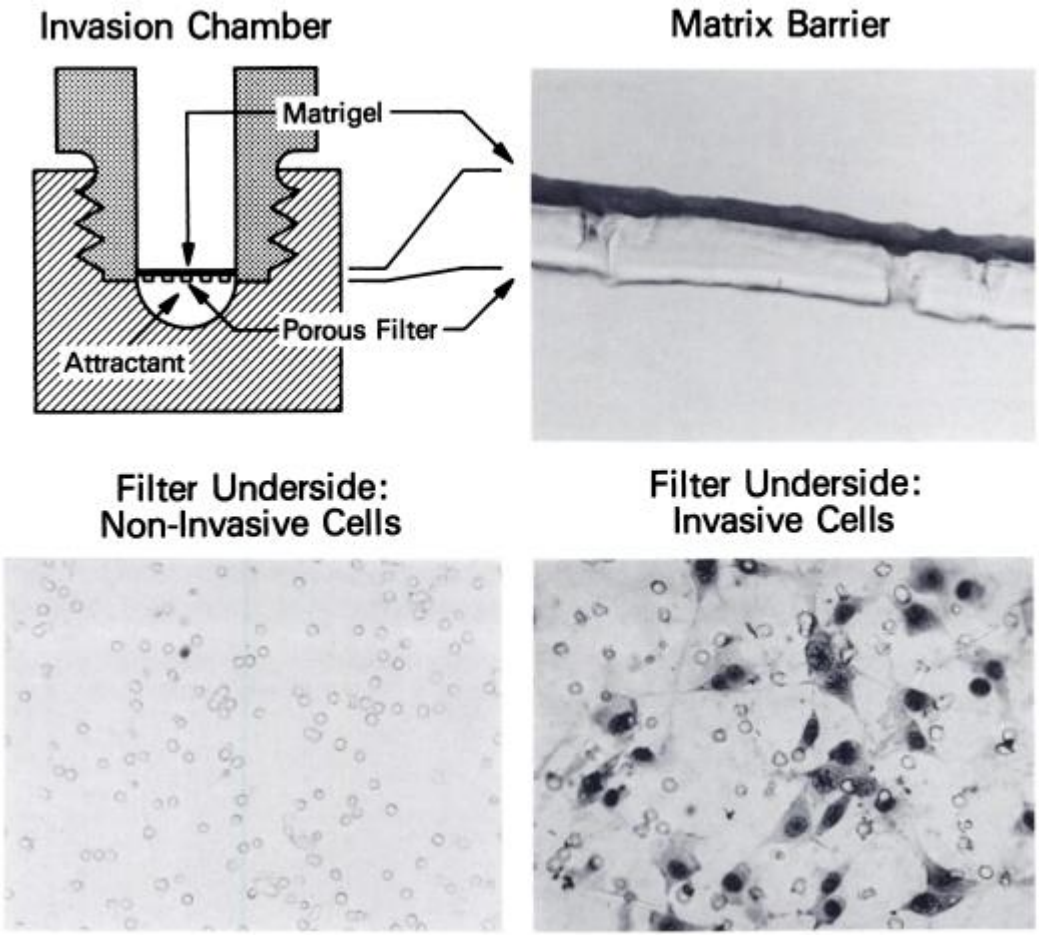

Figure 30. (From Albini, 1987). **Invasion assay**: Boyden chamber assembly used for the invasion assay is shown in the *upper left*; section of a matrigel-coated (50 ug protein) filter is shown in the *upper right*; lower surfaces of an invasion membrane when NIH 3T3 (*lower left*) and T24/3T3 (*lower right*) are assayed for invasion.

Effect of gene duplications on mast cell proliferation

Our hypothesis was that Shar-Pei MCTs with higher copy numbers would have increased mitotic indices due to stimulation of cell proliferation by increased HA in the extracellular matrix. We found that MCTs with greater than or equal to 7 mitoses per 10 hpf had a significantly higher median copy number

than MCTs with less than 7 mitoses per 10 hpf; however, a linear correlation between these two continuous variables was not found (data not shown). The use of other, potentially more representative, proliferation indices have been discussed above. In vitro quantification of proliferation in Shar-Pei MCTs, would provide another means of investigating the relationship between copy number and MCT proliferation.

Hyaluronan is known to stimulate the proliferation of mature, non-neoplastic, bone-marrow-derived mast cells by binding CD44 on the cell surface (Takano, 2009). Cell proliferation, measured by radioactive thymidine uptake, was decreased in murine $CD44^{-/-}$ mast cells and was decreased in $CD44^{+/+}$ mast cells in the presence of an anti-CD44 antibody, which blocked HA binding to CD44 (Takano, 2009). HA binding to CD44 also stimulates proliferation of human and bovine endothelial cells (Lokeshwar, 1996; Savani, 2001), and human melanoma cells (Ahrens, 2001). Greater than 80% of murine mammary carcinoma cells that were unable to bind HA to cell surface CD44 underwent apoptosis in a study of pulmonary metastasis, versus <20% of carcinoma cells possessing stable cell surface CD44 capable of binding HA (Yu, 1997). HA and CD44 also promotes tumor growth by reducing Fas expression and Fas-mediated apoptosis of human lung cancer cell lines (Yasuda, 2001). Since we know that cultured dermal fibroblasts from Shar-Pei dogs with higher copy numbers produce more HA, the question that remains is: “Do neoplastic mast cells of known copy number from Shar-Pei dogs display differential proliferation related to the HA content of their microenvironment?”

To investigate this relationship, cell lines of neoplastic mast cells from Shar-Pei dogs with known copy numbers would need to be cultivated as described above (Ohmori, 2008; London, 1996). Then a fixed number of cells from each cell line would be cultured in a 96-well plate containing media of varying HA concentrations for up to 120 hours, similar to previous studies (Ohmori, 2008; Yee, 1994). Cell viability would be assessed by trypan blue exclusion (Louis, 2011; Yee, 1994; London, 1996). Cell

proliferation would then be measured by direct visual cell counting with a hemocytometer or by quantification of nucleic acid content with cyanine dyes, such as PicoGreen (Quent, 2010). We predict that neoplastic mast cells grown in higher concentrations of HA would proliferate more rapidly. While Takano and colleagues (2012) described increased murine mast cell proliferation in hyaluronan-deficient media and no effect of exogenous HA on proliferation, which is contrast to the CD44 studies above and our proposed pathogenesis, their study used non-neoplastic mast cells, which may have altered mitogenic pathways compared to neoplastic mast cells.

Molecular weight of HA in cutaneous mucinosis

Another interesting component of the puzzle that requires further investigation is the molecular weight of the hyaluronan in Shar-Pei skin, as this has not been determined to the best of our knowledge. Most studies reporting the effects of HA do not report the molecular weight of HA polymers used, which would greatly enhance the implications of their work. The potential implications of determining the molecular weight of HA in Shar-Pei dogs are profound, as high-molecular-weight HA (1) is the major product of the HAS2 enzyme (Itano, 1999), shown to be upregulated in Shar-Pei fibroblasts (Zanna, 2009), (2) is implicated in hydrophilic expansion of the extracellular matrix (Comper, 1978), (3) has contradictory effects on angiogenesis and endothelial cell proliferation (stimulatory in Lokeshwar, 1996; inhibitory at high concentrations in West, 1989), and (4) inhibits cell cycle progression by inhibiting GTP loading of Rac and cyclin D1 signalling (Kothapalli, 2008). Low-molecular-weight HA is the result of partial degradation by hyaluronidases (Itano, 2011), which are not upregulated in Shar-Pei fibroblasts (Zanna, 2009), and it (1) stimulates cell cycle progression by stimulating ERK-dependent cyclin D1 expression (Kothapalli, 2008), (2) stimulates angiogenesis (Lokeshwar, 1996; West, 1989), (3) stimulates differentiation of monocytes into tumor-associated macrophages (McKee, 1996), and (4) downregulates

Fas-mediated apoptosis by binding CD44 (Yasuda, 2001). Additionally, low molecular weight HA, but not high molecular weight HA, is shown to be proinflammatory (McKee, 1996), and may contribute to the autoinflammatory disease Familial Shar-Pei Fever. Therefore, determination of the molecular weight of HA predominant in Shar-Pei would shed light on potential mechanisms of disease and cancer development.

Potential role of CD44 in biological behavior of Shar-Pei MCTs

As alluded to earlier, CD44 plays a major role in mediating hyaluronan-induced cellular signaling as the major cell surface receptor for HA (Knudson, 1996; Itano, 2011). Upon binding to extracellular HA, the transmembrane CD44 molecule undergoes cleavage, generating an intracellular domain that acts as a cell signal transduction molecule (Nagano, 2004). CD44 is integral to the homing of bone-marrow derived mast cells to the skin in mice, and is involved in terminal differentiation upon arrival (Takano, 2009). In vitro proliferation of murine mast cells was significantly suppressed by the administration of the anti-CD44 antibody, KM81 (Takano, 2009). CD44 on cancer cells binds hyaluronan to promote cell proliferation and motility via the Ras-MAP kinase and PI3 kinase-Akt pathways (Itano, 2011). Increased CD44 expression by tumor cells was seen in a study of canine malignant melanomas, with less intense expression in benign melanomas (Serra, 2004). HA binding to CD44 also stimulates proliferation of human and bovine endothelial cells (Lokeshwar, 1996; Savani, 2001), and human melanoma cells (Ahrens, 2001), and protects against apoptosis (Yu, 1997; Yasuda, 2001). In addition to contributing to cell proliferation, CD44 recruits matrix metalloproteinase 9 to the cell surface, promoting degradation of collagen IV invasion of vascular basement membranes (Yu, 1998). Thus, if the overproduction of dermal HA is not shown to be the main factor in the development of higher-grade MCTs in Shar-Pei dogs upon further investigation, the potential for upregulation and increased expression of CD44 on the surface of

neoplastic mast cells should be explored. In summary, our data suggest a relationship between HAS2 gene duplications and features of MCT aggressiveness in Shar-Pei dogs, but the exact mechanism has not been elucidated.

CONCLUSIONS

With the increasing use of molecular methods, such as polymerase chain reaction (PCR), to dissect the canine genome, researchers are becoming more aware of the genetic bases of phenotypic changes and breed-associated diseases. The causes of Familial Shar-Pei Fever and cutaneous mucinosis are being investigated, especially in Chinese Shar-Pei dogs displaying the meatmouth phenotype of excessive skin folding and a swollen muzzle. Familial Shar-Pei Fever is an autoimmune inflammatory disease that typically involves sporadic recurrent fevers and joint inflammation. Recurrent and prolonged systemic inflammation predisposes the patient to renal amyloidosis, which can result in renal failure. Shar-Pei Fever is linked to cutaneous mucinosis because both are associated with gene duplications upstream of the HAS2 gene, and subsequent overexpression of HAS2, resulting in excessive hyaluronan in the skin. This leads to cutaneous mucinosis and pronounced wrinkling of the skin.

This excessive hyaluronan may also impact the health of the Shar-Pei by promoting tumor cell motility and angiogenesis, resulting in more aggressive tumors. The relationship between dermal hyaluronan levels and the *risk* of MCT development is unknown, but if MCTs in Shar-Pei are more aggressive because of higher HAS2 gene expression and dermal hyaluronan, this may lead to the development of diagnostic tests that may more accurately predict MCT behavior in the Shar-Pei. Knowledge of a genetic basis for breed-associated diseases may also positively impact future breeding practices to preserve the integrity and health of the Chinese Shar-Pei breed for generations to come. In addition, the knowledge acquired from this study on the molecular basis of tissue hyaluronan's effects on MCT behavior may be able to be broadly applied to a variety of tumors in all dog breeds. Finally, the study may also promote investigation of novel therapeutic agents that may block the cancer-promoting actions of hyaluronan, such as the injectible hyaluronidase drugs Hydase and Hylenex, or 4-methylumbelliferone, an HA synthesis inhibitor, all used therapeutically in humans.

REFERENCES

1. Ahrens, T., V. Assmann, et al. (2001). CD44 is the Principal Mediator of Hyaluronic-Acid-Induced Melanoma Cell Proliferation. *Journal of Investigative Dermatology* **116**(1): 93-101.

2. Albini, A., Y. Iwamoto, et al. (1987). A Rapid *in Vitro* Assay for Quantitating the Invasive Potential of Tumor Cells. *Cancer Research* **47**: 3239-3245.

3. Alvarez, C.E., and J.M. Akey. (2012). Copy number variation in the domestic dog. *Mammalian Genome*. **23**: 144-163.

4. Barbosa, D.F.L., L.H. Pulz, et al. (2013). Microvessel Density is as a prognostic factor in canine cutaneous mast cell tumors. *BMC Proceedings* **7**(Suppl 2): 62.

5. Bostock, D.E., J. Crocker, et al. (1989). Nucleolar organizer regions as indicators of post-surgical prognosis in canine spontaneous mast cell tumours. *British Journal of Cancer* **59**: 915-918.

6. Bustin, S.A., V. Benes, et al. (2009). The MIQE Guidelines: *M*inimum *I*nformation for Publication of *Q*uantitative Real-Time PCR *E*xperiments. *Clinical Chemistry* **55**(4): 611-622.

7. Clemente, M., M.D. Perez-Alenza, et al. (2010). Histological, Immunohistological, and Ultrastructural Description of Vasculogenic Mimicry in Canine Mammary Cancer. *Veterinary Pathology* **47**(2): 265-274.

8. Comper, W.D., and T.C. Laurent. (1978). Physiological Function of Connective Tissue Polysaccharides. *Physiological Reviews* **58**(1): 255-315.

9. DeVinney, R., and W.M. Gold. (1990). Establishment of Two Dog Mastocytoma Cell Lines in Continuous Culture. *American Journal of Respiratory Cell and Molecular Biology* **3**: 413-420.

10. D'haene, B., J. Vandesompele, and J. Hellemans. Accurate and objective copy number profiling using real-time quantitative PCR. *Methods* **50**: 262-270.

11. Docampo, M. J., G. Zanna, et al. (2011). Increased HAS2-driven hyaluronic acid synthesis in shar-pei dogs with hereditary cutaneous hyaluronosis (mucinosis). *Veterinary Dermatology* **22**(6): 535-545.

12. Doliger, S., M. Delverdier, et al. (1995). Histochemical Study of Cutaneous Mucins in Hypothyroid Dogs. *Veterinary Pathology* **32**: 628-634.

13. Downs, T.R., and W.W. Wilfinger. (1983). Fluorometric Quantification of DNA in Cells and Tissue. *Analytical Biochemistry* **131**: 538-547.

14. Elston, L. B., F. A. R. Sueiro, et al. (2009). The Importance of the Mitotic Index as a Prognostic Factor for Survival of Canine Cutaneous Mast Cell Tumors: A Validation Study. *Veterinary Pathology* **46**(2): 362-364.

15. Fox, S.B., R.D. Leek, et al. (1995). Quantitation and prognostic value of breast cancer angiogenesis: Comparison of microvessel density, Chalkley count, and computer image analysis. *Journal of Pathology* **177**(3): 275-283.

16. Hansen, S., D.A. Grabau, et al. (1998). Angiogenesis in breast cancer: a comparative study of the observer variability of methods for determining microvessel density. *Laboratory Investigation* **78**(12): 1563-1573.

17. Hansen, S., F.B. Sorensen, et al. (2004). Microvessel density compared with Chalkley count in a prognostic study of angiogenesis in breast cancer patients. *Histopathology* **44**: 428-436.

18. Hansen, T.F., F.B. Sorensen, et al. (2010). Microvessel density and the association with single nucleotide polymorphisms of the vascular endothelial growth factor receptor 2 in patients with colorectal cancer. *Virchows Archives* **456**: 251-260.

19. Ishiguro, T., T. Kadosawa, et al. (2001). Establishment and Characterization of a New Canine Mast Cell Tumor Cell Line. *Journal of Veterinary Medical Science* **63**(9): 1031-1034.

20. Itano, N., T. Sawai, et al. (1999). Three Isoforms of Mammalian Hyaluronan Synthases Have Distinct Enzymatic Properties. *Journal of Biological Chemistry* **274**(35): 25085-25092.

21. Itano, N. (2011). Hyaluronan: A Key Microenvironmental Mediator of Tumor-Stromal Cell Interactions. *Tumor-Associated Fibroblasts and their Matrix*. M. M. Mueller and N. E. Fusenig, Springer Netherlands. **4:** 127-144.

22. Jennings, R.N., M.A. Miller, and J.A. Ramos-Vara. (2012). Comparison of CD34, CD31, and Factor VIII-Related Antigen Immunohistochemical Expression in Feline Vascular Neoplasms and CD34 Expression in Feline Nonvascular Neoplasms. *Veterinary Pathology* **49**(3): 532-537.

23. Kim, C., S. Chung, et al. (2012). *In vitro* angiogenesis assay for the study of cell-encapsulation therapy. *Lab Chip* **12**: 2942-2950.

24. Kiupel, M., J. D. Webster, et al. (2005). Impact of Tumour Depth, Tumour Location and Multiple Synchronous Masses on the Prognosis of Canine Cutaneous Mast Cell Tumours. *Journal of Veterinary Medicine* **52**(6): 280-286.

25. Kiupel, M., J. D. Webster, et al. (2011). Proposal of a 2-Tier Histologic Grading System for Canine Cutaneous Mast Cell Tumors to More Accurately Predict Biological Behavior. *Veterinary Pathology* **48**(1): 147-155.

26. Knudson, W. (1996). Tumor-Associated Hyaluronan. *American Journal of Pathology* **148**(6): 1721-1726.

27. Kohlberger, P.D., A. Obermair, et al. (1996). Quantitative immunohistochemistry of factor VIII-related antigen in breast carcinoma: a comparison f computer-assisted image analysis with established counting methods. *American Journal of Clinical Pathology* **105**(6): 705-710.

28. Koothapalli, D., J. Flowers, et al. (2008). Differential Activation of ERK and Rac Mediates the Proliferative and Anti-proliferative Effects of Hyaluronan. *Journal of Biological Chemistry* **283**(46): 31823-31829.

29. Lavalle, G.E., A.C. Bertagnolli, et al. (2009). Cox-2 Expression in Canine Mammary Carcinomas: Correlation with Angiogenesis and Overall Survival. *Veterinary Pathology* **46**: 1275-1280.

30. Lazarus, S.C., R. DeVinney, et al. (1986). Isolated canine mastocytoma cells: propagation and characterization of two cell lines. *American Journal of Physiology* **251**(6): C935-944.

31. Lehmann, U., and H. Kreipe. (2001). Real-Time PCR Analysis of DNA and RNA Extracted from Formalin-Fixed and Parafin-Embedded Biopsies. *Methods* **25**: 409-418.

32. Lenth, R. V. (2006-9). Java Applets for Power and Sample Size [Computer software]. Retrieved Sept 1, 2012, from http://www.stat.uiowa.edu/~rlenth/Power.

33. Lin, T.-Y., R. Thomas, et al. (2009). Generation and characterization of novel canine malignant mast cell line CL1. *Veterinary Immunology and Immunopathology* **127**: 114-124.

34. Liu, J., Y. Zhang, et al. (2011). Mast cell: insight into remodeling a tumor microenvironment. *Cancer Metastasis Review* **30**: 177-184.

35. Livak, K.J., and T.D. Schmittgen. (2001). Analysis of Relative Gene Expression Data Using Real-Time Quantitative PCR and the 2-[Delta][Delta]CT Method. *Methods* **25**(4): 402-408.

36. Lokeshwar, V.B., N. Iida, and L.Y.W. Bourguignon. (1996). The Cell Adhesion Molecule, GP16, Is a New CD44 Variant (ex14/v10) Involved in Hyaluronic Acid Binding and Endothelial Cell Proliferation. *Journal of Biological Chemistry* **271**(39): 23853-23864.

37. London, C.A., W.C. Kisseberth, et al. (1996). Expression of Stem Cell Factor Receptor (c-*kit*) by the Malignant Mast Cells from Spontaneous Canine Mast Cell Tumours. *Journal of Comparative Pathology* **115**: 399-414.

38. Lopez, A., D. Spracklin, et al. (1999). Cutaneous mucinosis and mastocytosis in a shar-pei. *Canadian Veterinary Journal* **40**(12): 881-883.

39. Louis, K.S., and A.C. Siegel. (2011). Cell Viability Analysis Using Trypan Blue: Manual and Automated Methods. *Methods in Molecular Biology*. M.J. Stoddart (ed.). Springer. **740**: 7-12.

40. Luong, R. H., K. E. Baer, et al. (2006). Prognostic Significance of Intratumoral Microvessel Density in Canine Soft-Tissue Sarcomas. *Veterinary Pathology Online* **43**(5): 622-631.

41. Maiolino, P., M. Cataldi, et al. (2005). Nucleomorphometric Analysis of Canine Cutaneous Mast Cell Tumours. *Journal of Comparative Pathology* **133**(2-3): 209-211.

42. McKee, C.M., M.B. Penno, et al. (1996). Hyaluronan (HA) Fragments Induce Chemokine Gene Expression in Alveolar Macrophages. *Journal of Clinical Investigation* **98**(10): 2403-2413.
43. Miller, D. R. (1995). The occurrence of mast cell tumors in young Shar-Peis. *Journal of Veterinary Diagnostic Investigation* **7**(3): 360-363.

44. Mukaratirwa, S., M. Chimonyo, et al. (2004). Stromal cells and extracellular matrix components in spontaneous canine transmissible venereal tumour at different stages of growth. *Histology and Histopathology* **19**(4): 1117-1123.

45. Mukaratirwa, S., A. M. van Ederen, et al. (2004). Versican and hyaluronan expression in canine colonic adenomas and carcinomas: Relation to malignancy and depth of tumour invasion. *Journal of Comparative Pathology* **131**(4): 259-270.

46. Nagano, O., and H. Saya. (2004). Mechanism and biological significance of CD44 cleavage. *Cancer Science* **95**(12): 930-935.

47. Northrup, N. C., E. W. Howerth, et al. (2005). Variation among pathologists in the histologic grading of canine cutaneous mast cell tumors with uniform use of a single grading reference. *Journal of Veterinary Diagnostic Investigation* **17**(6): 561-564.

48. Ohmori, K., S. Kawarai, et al. (2008). Identification of c-*kit* mutations-independent neoplastic cell proliferation of canine mast cells. *Veterinary Immunology and Immunopathology* **126**: 43-53.

49. Olsson, M., J. R. S. Meadows, et al. (2011). A Novel Unstable Duplication Upstream of HAS2 Predisposes to a Breed-Defining Skin Phenotype and a Periodic Fever Syndrome in Chinese Shar-Pei Dogs. *PLoS Genetics* **7**(3).

50. Pasonen-Seppanen, S, P. Takabe, et al. (2012). Melanoma cell-derived factors stimulate hyaluronan synthesis in dermal fibroblasts by upregulating HAS2 through PDGFR-PI3K-AKT and p38 signaling. *Histochemical Cell Biology* **138**: 895-911.

51. Passantino, L., G. Passantino, et al. (2008). Expression of Proto-Oncogene C-kit and Correlation with Morphological Evaluations in Canine Cutaneous Mast Cell Tumors. *Immunopharmacology and Immunotoxicology* **30**(3): 609-621.

52. Patnaik, A. K., W. J. Ehler, et al. (1984). Canine Cutaneous Mast Cell Tumor: Morphologic Grading and Survival Time in 83 Dogs. *Veterinary Pathology* **21**(5): 469-474.

53. Pennington, D.W., A.R. Lopez, et al. Dog Mastocytoma Cells Produce Transforming Growth Factor $Beta_1$. *Journal of Clinical Investigation* **90**: 35-41.

54. Poggiani, S.dS.C., E.M. Terra, et al. (2012). Canine Cutaneous Mast Cell Tumor: Biologic Behavior and Its Correlation with Prognostic Indicators. *Open Journal of Veterinary Medicine* **2**: 255-261.

55. Preziosi, R., G. Sarli, et al. (2004). Prognostic Value of Intratumoral Vessel Density in Cutaneous Mast Cell Tumours of the Dog. *Journal of Comparative Pathology* **130**(2-3): 143-151.

56. Preziosi, R., G. Sarli, et al. (2007). Multivariate Survival Analysis of Histological Parameters and Clinical Presentation in Canine Cutaneous Mast Cell Tumours. *Veterinary Research Communications* **31**(3): 287-296.
57. Pusztaszeri, M.P., W. Seelentag, and F.T. Bosman. (2006). Immunohistochemical Expression of Endothelial Markers CD31, CD34, von Willebrand Factor, and Fli-1 in Normal Human Tissues. *Journal of Histochemistry & Cytochemistry* **54**(4): 385-395.

58. Quent, V.M.C., D. Loessner, et al. (2010). Discrepancies between metabolic activity and DNA content as tool to assess cell proliferation in cancer research. *Journal of Cellular and Molecular Medicine* **14**(4): 1003-1013.

59. Rago, R., J. Mitchen, and G. Wilding. (1990). DNA Fluorometric Assay in 96-Well Tissue Culture Plates Using Hoechst 33258 after Cell Lysis by Freezing in Distilled Water. *Analytical Biochemistry* **191**: 31-34.

60. Romansik, E. M., C. M. Reilly, et al. (2007). Mitotic Index is Predictive for Survival for Canine Cutaneous Mast Cell Tumors. *Veterinary Pathology* **44**(3): 335-341.

61. Ropponen, K., M. Tammi, et al. (1998). Tumor cell-associated hyaluronan as an unfavorable prognostic factor in colorectal cancer. *Cancer Research* **58**(2): 342-347.

62. Saito, T., T. Dai, and R. Asano. (2013). The hyaluronan synthesis inhibitor 4-methylumbelliferone exhibits antitumor effects against mesenchymal-like canine mammary tumor cells. *Oncology Letters* **5**: 1068-1074

63. Savani, R.C., G. Cao, et al. (2001). Differential Involvement of the Hyaluronan (HA) Receptors CD44 and Receptor for HA-mediated Motility in Endothelial Cell Function and Angiogenesis. *Journal of Biological Chemistry* **276**(39): 36770-36778.

64. Scase, T.J., D. Edwards, et al. (2006). Canine Mast Cell Tumors: Correlation of Apoptosis and Proliferation Markers with Prognosis. *Journal of Veterinary Internal Medicine* **20**: 151-158.

65. Serra, M., R.M. Rabanal, et al. (2004). Differential Expression of CD44 in Canine Melanocytic Tumours. *Journal of Comparative Pathology* **130**: 171-180.

66. Sfiligoi, G., K. M. Rassnick, et al. (2005). Outcome of dogs with mast cell tumors in the inguinal or perineal region versus other cutaneous locations: 124 cases (1990-2001). *Journal of the American Veterinary Medical Association* **226**(8): 1368-1374.

67. Simoes, J. P. C., P. Schoning, and M. Butine. (1994). Prognosis of Canine Mast Cell Tumors: A Comparison of Three Methods. *Veterinary Pathology* **31**(6): 637-647.

68. Sleeckx, N., L. Van Brantegem, et al. (2013). Evaluation of Immunohistochemical Markers of Lymphatic and Blood Vessels in Canine Mammary Tumours. *Journal of Comparative Pathology* **148**: 307-317.

69. Strefezzi, R. D., J. G. Xavier, et al. (2003). Morphometry of Canine Cutaneous Mast Cell Tumors. *Veterinary Pathology* **40**(3): 268-275.

70. Sugiyama, Y., A. Shimada, et al. (1998). Putative Hyaluronan Synthase mRNA Are Expressed in Mouse Skin and TGF-[beta] Upregulates Their Expression in Cultured Human Skin Cells. *Journal of Investigative Dermatology* **110**(2): 116-121.

71. Takano, H., S. Nakazawa, et al. (2009). Involvement of CD44 in mast cell proliferation during terminal differentiation. *Laboratory Investigation* **89**(4): 446-455.

72. Takano, H., K. Furuta, et al. (2012). Restriction of Mast Cell Proliferation through Hyaluronan Synthesis by Co-cultured Fibroblasts. *Biological Pharmaceutical Bulletin* **35**(3) 408-412.

73. Thompson, J. J., D. L. Pearl, et al. (2011). Canine Subcutaneous Mast Cell Tumor: Characterization and Prognostic Indices. *Veterinary Pathology* **48**(1): 156-168.

74. Toole, B. P. and M. G. Slomiany (2008). Hyaluronan: A constitutive regulator of chemoresistance and malignancy in cancer cells. *Seminars in Cancer Biology* **18**(4): 244-250.

75. Walter, G., W. Zillig, et al. (1967). Initiation of DNA-Dependent RNA Synthesis and the Effect of Heparin on RNA Polymerase. *European Journal of Biochemistry* **3**(2): 194-201.

76. Webster, J.D., M.M. Dennis, et al. (2011). Recommended Guidelines for the Conduct and Evaluation of Prognostic Studies in Veterinary Oncology. *Veterinary Pathology* **48**(1): 7-18.

77. Weidner, N., J.P. Semple, et al. (1991). Tumor Angiogenesis and Metastasis – Correlation in Invasive Breast Carcinoma. *New England Journal of Medicine* **324**(1): 1-8.

78. Welle, M., S. Grimm, et al. (1999). Mast Cell Density and Subtypes in the Skin of Shar Pei Dogs with Cutaneous Mucinosis. *Journal of Veterinary Medicine* **46**: 309-316.

79. Welle, M. M., C. R. Bley, et al. (2008). Canine mast cell tumours: a review of the pathogenesis, clinical features, pathology and treatment. *Veterinary Dermatology* **19**(6): 321-339.

80. West, D.C., and S. Kumar. (1989). The Effect of Hyaluronate and Its Oligosaccharides on Endothelial Cell Proliferation and Monolayer Integrity. *Experimental Cell Research* **183**: 179-196.

81. Wild, R., S. Ramakrishnan, et al. (2000). Quantitative Assessment of Angiogenesis and Tumor Vessel Architecture by Computer-Assisted Digital Image Analysis: Effects of VEGF-Toxin Conjugate on Tumor Microvessel Density. *Microvascular Research* **59**: 368-376.

82. Wolf, K., I. Mazo, et al. (2003). Compensation mechanism in tumor cell migration: mesenchymal-amoeboid transition after blocking of pericellular proteolysis. *Journal of Cell Biology* **160**(2): 267-277.

83. Yasuda, M., Y. Tanaka, et al. (2001). CD44 stimulation down-regulates Fas expression and Fas-mediated apoptosis of lung cancer cells. *International Immunology* **13**(10): 1309-1319.

84. Yee, N.S., I. Paek, and P. Besmer. (1994). Role of *kit*-Ligand in Proliferation and Suppression of Apoptosis in Mast Cells: Basis for Radiosensitivity of *White Spotting* and *Steel* Mutant Mice. *Journal of Experimental Medicine* **179**: 1777-1787.

85. Yu, Q., B.P. Toole, and I. Stamenkovic. (1997). Induction of Apoptosis of Metastatic Mammary Carcinoma Cells In Vivo by Disruption of Tumor Cell Surface CD44 Function. *Journal of Experimental Medicine* **186**(12): 1985-1996.

86. Yu, Q., and I. Stamenkovic. (1999). Localization of matrix metalloproteinase 9 to the cell surface provides a mechanism for CD44-mediated tumor invasion. *Genes & Development* **13**: 35-48.

87. Zanna, G., D. Fondevila, et al. (2008). Cutaneous mucinosis in shar-pei dogs is due to hyaluronic acid deposition and is associated with high levels of hyaluronic acid in serum. *Veterinary Dermatology* **19**(5): 314-318.

88. Zanna, G., M. J. Docampo, et al. (2009). Hereditary cutaneous mucinosis in shar pei dogs is associated with increased hyaluronan synthase-2 mRNA transcription by cultured dermal fibroblasts. *Veterinary Dermatology* **20**(5-6): 377-382.

APPENDIX 1. TABLE OF RESULTS FROM NORMAL NON-SHAR-PEI SKIN

Normal non-Shar-Pei skin

Case	M1 copy number	T1 copy number	Avg copy number	Histo mucin score
001-35233	ND	ND	ND	0
001-35722	4.89	4.05	4.47	0
023-24446	2.88	2.31	2.595	0
023-38833	ND	ND	ND	0
045-70036	2.95	4.66	3.805	0
067-26824	ND	ND	ND	0
090-00184	ND	ND	ND	0
090-07283	ND	ND	ND	1
090-14760	ND	ND	ND	0
090-31313	ND	ND	ND	0
090-42215	ND	ND	ND	0

ND = not determined

APPENDIX 2. TABLE OF RESULTS FROM NORMAL SHAR-PEI SKIN

Normal Shar-Pei skin

Case	M1 copy number	T1 copy number	Avg copy number	Histo mucin score
001-31421	6.02	6.45	6.235	2
001-52855	6.73	7.06	6.895	2
001-54796	ND	ND	ND	2
012-04283	3.89	5.78	4.835	1
034-75345	14.03	10.41	12.22	0
045-15457	6.96	7.21	7.085	3
045-36577	34.54	9.78	22.16	1
045-41528	25.46	11.24	18.35	0
067-02763	6.77	10.41	8.59	3
067-61551	22.63	15.03	18.83	3
067-77261	25.63	13.36	19.495	1
078-07024	ND	ND	ND	2
090-43375	23.43	11.63	17.53	2

ND = not determined

APPENDIX 3. TABLE OF RESULTS FROM SHAR-PEI MCT-ADJACENT SKIN

Shar-Pei MCT-adjacent skin

Case	M1 copy number	T1 copy number	Avg copy number	Histo mucin score
001-57537	7.62	15.12	11.37	1
012-18032	4.69	0.69	2.69	1
012-57599	13.18	11.93	12.555	1
023-00376	5.66	19.56	12.61	2
023-14042	4.69	11	7.845	3
023-53902	3.95	7.67	5.81	1
023-58795	8.11	9.13	8.62	3
034-45524	10.78	13	11.89	3
034-69390	12.61	10.47	11.54	2
045-01156	24.59	17.88	21.235	3

APPENDIX 4. TABLE OF RESULTS FROM SHAR-PEI MCTS

Shar-Pei MCTs

Case	Patnaik Grade	Kiupel Grade	M1 Copy #	T1 Copy #	Avg Copy #	Mucin score	Mitotic Index	MVD hand	MVD comp	Depth of Invasion
001-05894	1	low	ND	ND	ND	1	0	ND	ND	1
001-10950	3	high	13.64	14.42	14.03	3	17	129	185	3
001-12345	2	low	7.11	17.44	12.275	2	0	ND	ND	3
001-14672	2	high	8.06	5.5	6.78	1	9	ND	ND	3
001-18045	2	high	13.18	12.64	12.91	3	10	ND	ND	2
001-19071	2	low	7.65	9.21	8.43	1	0	ND	ND	2
001-20307	3	high	ND	ND	ND	1	18	191	161	2
001-21898	2	high	9.75	19.28	14.515	3	5	ND	ND	2
001-23662	2	high	ND	ND	ND	3	1	ND	ND	1
001-26096	1	low	5.13	6.32	5.725	2	0	ND	ND	1
001-27003	3	high	ND	ND	ND	2	39	80	181	3
001-33973	3	high	ND	ND	ND	3	20	131	190	3
001-47765	3	high	ND	ND	ND	1	31	129	157	3
001-48032	3	high	4.47	8.94	6.705	2	9	ND	ND	3
001-49742	3	high	7.31	11.88	9.595	3	12	ND	ND	3
001-55072	2	low	1.28	6.02	3.65	0	0	81	159	3
001-56404	2	low	1.72	6.73	4.225	1	0	91	339	3
001-57537	3	high	8.46	12.79	10.625	1	37	ND	ND	2
001-62837	2	low	12.3	14.72	13.51	3	0	ND	ND	3
001-65925	2	high	7.95	11.63	9.79	1	15	ND	ND	3
012-05143	2	high	2.11	5.24	3.675	3	11	ND	ND	3
012-06949	2	low	15.14	19.16	17.15	1	2	ND	ND	3
012-08738	3	high	10.13	9.25	9.69	3	4	ND	ND	3
012-18032	2	low	4.29	7.8	6.045	3	3	143	339	3
012-19579	2	high	1.67	2.69	2.18	1	2	ND	ND	3
012-24763	3	high	45.26	27.47	36.365	1	43	161	292	3
012-29219	3	high	12.73	10.93	11.83	1	91	ND	ND	3
012-30480	3	high	ND	ND	ND	3	32	ND	ND	3
012-33408	2	high	8.69	8.06	8.375	2	11	ND	ND	3
012-33575	3	high	9.78	13.64	11.71	1	36	ND	ND	3
012-35595	2	low	3.95	6.82	5.385	1	2	102	113	3
012-36085	3	high	3.56	7.95	5.755	2	4	ND	ND	3
012-38329	2	low	2.87	7.16	5.015	1	1	62	101	3

012-44353	3	high	6.41	11.31	8.86	1	42	ND	ND	3
012-44425	2	low	6.11	9.25	7.68	3	0	ND	ND	3
012-51125	2	high	ND	ND	ND	0	9	133	187	3
012-55421	2	high	2.68	13	7.84	3	11	ND	ND	2
012-57599	3	high	5.28	10.57	7.925	3	7	109	99	3
012-64781	2	low	11.08	8	9.54	2	0	ND	ND	3
012-65244	2	high	12.64	9.71	11.175	3	28	ND	ND	3
012-71360	3	high	ND	ND	ND	0	33	ND	ND	3
023-06483	3	high	ND	ND	ND	1	168	ND	ND	3
023-14042	2	low	6.58	8.14	7.36	3	0	89	165	3
023-28373	3	high	ND	ND	ND	3	37	ND	ND	3
023-45044	2	low	1.08	3.95	2.515	2	1	ND	ND	3
023-45917	3	high	8.22	8.75	8.485	0	39	ND	ND	3
023-50217	2	low	ND	ND	ND	3	0	ND	ND	3
023-53902	2	low	3.41	4.76	4.085	1	2	58	111	3
023-58795	2	low	12.73	13.27	13	3	0	ND	ND	3
034-02407	2	low	ND	ND	ND	2	1	ND	ND	3
034-04520	3	high	25.46	14.72	20.09	1	47	124	167	3
034-07018	2	high	ND	ND	ND	0	11	ND	ND	3
034-13281	3	high	ND	ND	ND	0	15	ND	ND	3
034-20940	1	low	12.64	14.72	13.68	1	2	ND	ND	2
034-23336	3	high	ND	ND	ND	3	78	ND	ND	3
034-26019	2	low	ND	ND	ND	3	0	ND	ND	3
034-29680	2	low	29.24	18.25	23.745	3	4	385	185	3
034-35396	3	high	ND	ND	ND	1	72	ND	ND	3
034-35499	3	high	ND	ND	ND	0	9	ND	ND	3
034-45524	2	low	5.19	11.32	8.255	1	6	ND	ND	2
034-47918	2	low	ND	ND	ND	2	2	ND	ND	3
034-50134	3	high	13.36	10.78	12.07	2	2	183	135	2
034-53005	2	high	ND	ND	ND	3	7	ND	ND	2
034-55332	3	high	ND	ND	ND	2	26	ND	ND	3
034-60193	3	high	ND	ND	ND	2	7	ND	ND	3
034-67928	3	high	8.22	7.16	7.69	2	38	72	121	2
034-69370	3	high	ND	ND	ND	1	4	ND	ND	3
034-69390	2	low	9.36	11.74	10.55	3	0	120	107	3
034R02698	3	high	ND	ND	ND	0	7	ND	ND	3
045-01156	3	high	6.77	7.01	6.89	3	27	ND	ND	3
045-04164	3	high	ND	ND	ND	1	18	ND	ND	3
045-11237	2	low	14.12	15.24	14.68	1	0	76	173	3
045-12091	3	high	ND	ND	ND	3	59	ND	ND	3
045-12222	3	high	ND	ND	ND	1	41	ND	ND	3

045-22637	2	low	ND	ND	ND	1	0	ND	ND	3
045-31342	2	low	ND	ND	ND	3	0	ND	ND	3
045-36990	3	high	65.35	28.8	47.075	2	17	173	167	2
045-37724	2	high	ND	ND	ND	2	25	ND	ND	3
045-38996	3	high	32.67	17.89	25.28	1	53	115	167	3
045-40068	2	high	ND	ND	ND	0	16	ND	ND	2
045-44225	2	low	ND	ND	ND	1	0	ND	ND	3
045-46812	2	low	32.45	23.84	28.145	3	0	66	187	3
045-54292	2	high	ND	ND	ND	3	15	ND	ND	2
045-59491	2	low	32	32	32	1	0	148	113	3
045-71989	3	high	ND	ND	ND	2	8	ND	ND	3
045-74408	2	high	ND	ND	ND	3	2	ND	ND	1
045-78414	3	high	ND	ND	ND	1	26	ND	ND	3
056-03053	2	low	44.63	25.28	34.955	2	0	ND	ND	3
056-03814	2	low	36.25	19.7	27.975	3	0	93	111	2
056-04717	2	low	ND	ND	ND	3	4	ND	ND	3
056-07033	2	low	ND	ND	ND	2	0	ND	ND	3
056-16154	3	high	ND	ND	ND	2	44	ND	ND	3
056-24229	2	high	ND	ND	ND	1	0	ND	ND	3
056-25878	3	high	ND	ND	ND	3	38	ND	ND	3
056-36551	3	high	ND	ND	ND	3	61	ND	ND	3
056-51623	2	high	ND	ND	ND	3	50	ND	ND	2
056-53930	3	high	46.53	28.25	37.39	0	19	151	69	3
056-62151	2	low	ND	ND	ND	3	0	ND	ND	3
067-03650	1	low	ND	ND	ND	0	0	ND	ND	1
067-09419	3	high	17.15	11.63	14.39	2	36	115	137	3
067-15969	2	high	ND	ND	ND	3	8	ND	ND	3
067-27245	2	low	ND	ND	ND	2	0	ND	ND	3
067-29901	2	high	ND	ND	ND	2	5	ND	ND	3
067-31237	1	low	ND	ND	ND	3	0	ND	ND	1
067-31388	3	high	ND	ND	ND	2	22	ND	ND	3
067-36850	2	low	2.66	2.5	2.58	1	0	62	149	3
067-48279	2	high	ND	ND	ND	1	4	ND	ND	3
067-60101	1	low	ND	ND	ND	0	0	ND	ND	1
067-68149	1	low	ND	ND	ND	1	0	ND	ND	1
067-80824	2	low	ND	ND	ND	2	2	ND	ND	3
078-16481	2	low	60.13	31.78	45.955	3	0	ND	ND	2
078-16807	3	high	ND	ND	ND	1	21	ND	ND	3
078-19732	3	high	64.89	30.7	47.795	0	20	116	181	2
078-23725	3	high	6.92	5.62	6.27	0	62	77	298	3
078-32632	3	high	69.07	41.64	55.355	0	12	184	385	2

078-36872	2	low	ND	ND	ND	2	0	ND	ND	3
078-42087	2	low	ND	ND	ND	0	0	ND	ND	3
078-45694	3	high	51.63	29.45	40.54	1	7	125	169	2
078-58339	2	low	40.22	22.63	31.425	1	2	115	190	2
078-67093	2	low	8.63	15.45	12.04	1	0	ND	ND	2
078-67229	2	low	ND	ND	ND	3	1	66	147	3
078-84039	1	low	ND	ND	ND	3	0	ND	ND	1
089-02857	3	high	ND	ND	ND	1	36	ND	ND	3
089-17598	2	low	ND	ND	ND	1	0	ND	ND	3
089-26036	2	low	ND	ND	ND	2	1	151	317	2
089-28652	2	high	ND	ND	ND	3	1	ND	ND	3
089-28694	3	high	52.71	31.78	42.245	3	13	76	194	3
089-55821	2	low	32.9	32.45	32.675	2	1	70	190	3
089-56865	2	low	0.61	1.11	0.86	3	0	79	79	2
089-57623	3	high	10.7	13.64	12.17	3	15	83	165	3
089-64399	2	low	3.48	8	5.74	3	1	48	113	2
089-73248	3	high	ND	ND	ND	3	24	ND	ND	2
089-76265	2	low	ND	ND	ND	2	5	ND	ND	3
090-05787	2	high	ND	ND	ND	2	17	ND	ND	2
090-07823	3	high	ND	ND	ND	2	121	ND	ND	3
090-12347	2	high	ND	ND	ND	3	9	ND	ND	2
090-25480	2	high	ND	ND	ND	1	7	ND	ND	3
090-32619	2	low	ND	ND	ND	3	1	ND	ND	3
090-38460	2	high	ND	ND	ND	0	7	ND	ND	2
090-40434	3	high	ND	ND	ND	3	17	ND	ND	3
090-43127	3	high	7.11	45.89	26.5	0	24	79	85	3
090-46122	1	low	1.93	0.9	1.415	3	0	41	115	1
090-48198	3	high	ND	ND	ND	2	14	ND	ND	2
090-52731	2	low	ND	ND	ND	2	0	ND	ND	3
090-54127	2	low	ND	ND	ND	2	0	ND	ND	2
090-62059	3	high	36	22.16	29.08	2	27	105	161	3
090-64799	3	high	54.95	33.82	44.385	2	55	73	139	3
090-71331	3	high	15.78	29.86	22.82	3	17	104	137	3
990-54746	2	high	30.27	21.41	25.84	2	14	ND	ND	3

ND = not determined